



University of
Stavanger

FACULTY OF SCIENCE AND TECHNOLOGY

MASTER'S THESIS

Study programme/specialisation:

Master of Science, Biological Chemistry,
Specialization in Molecularbiology

Spring/ Autumn semester, 2020

Open

Author: Gorana Drobac

Programme coordinator:

Supervisor(s): Peter Ruoff

Title of master's thesis:

Homeostasis by depression kinetics with multisite inhibition and positive feedback

Credits: 60 ECTS

Keywords:

Biological chemistry, Computational biology,
Homeostasis, Kinetics, Controller motifs

Number of pages: 55

+ supplemental material/other: 9

Stavanger, 30/08/2020
date/year

UNIVERSITY OF STAVANGER

**Homeostasis by depression kinetics with
multisite inhibition and positive
feedback**

by

Gorana Drobac

Master Thesis in Biological Chemistry

submitted to the

Faculty of Science and Technology

Department of Biology, Chemistry and Environmental Engineering

August 2020

“Enthusiasm is common. Endurance is rare.”

Angela Duckworth

UNIVERSITY OF STAVANGER

Abstract

Faculty of Science and Technology
Department of Biology, Chemistry and Environmental Engineering

Master Thesis in Biological Chemistry

by Gorana Drobac

In order to survive all living organisms must, to some extent, be able to adapt to the changes in environment. In recent years there have been proposed different controller motifs that are used to explain how does the organisms achieve robust homeostasis. The most of the proposed controller motifs reach the limit when the perturbations become time dependent. Motifs based on depression kinetics have shown ability to keep up with the even exponential and hyperbolic change in perturbation. The only unfavorable with these controllers is that they tend to break down when the concentration of the regulatory inhibitor becomes too low and the compensatory flux has reached its maximum.

So, in order to circumvent this disadvantage we have included a multisite inhibition and positive feedback mechanism.

We have as well taken the time to test other abilities of the newly composed controller and showed that it can become oscillatory and still preserve the homeostasis by keeping the average concentration of controlled variable at the defined level.

Acknowledgements

Well, I must admit that writing this thesis was a great challenge giving that I never worked with computational biology. Although a challenge, I can say it was a journey worth taking because I learned a lot.

This journey would not be the same if I hadn't had the unconditional support of my supervisor Peter Ruoff. He was always there to answer my questions, to give helping hand and guidance and I am forever thankful for that.

I would also like to thank my husband for his support in this career defining moment. It was difficult, but we did it together.

Contents

Abstract	ii
Acknowledgements	iii
List of Figures	vi
1 Introduction	1
1.1 Homeostasis	1
1.2 Regulation of Homeostasis	2
1.3 Controller motif 2	5
1.4 Effect of multisite inhibition	7
1.5 Oscillatory homeostasis	9
2 Aim of thesis	11
3 Methods	12
4 Results and Discussion	13
4.1 Influence of K_I on the controller performance	13
4.2 Implementation of multisite inhibition	14
4.3 Increasing controller lifetime by increasing the maximum compensatory flux	15
4.4 Implementing the positive feedback activation of C in order to stop the controller breakdown	18
4.4.1 First order autocatalysis in C	19
4.4.2 Second order autocatalysis in C	22
4.5 Oscillatory homeostasis	25
4.5.1 Time dependent perturbations for controller motif 2	26
4.5.2 Time dependent perturbation of controller motif 2 with C	29
5 Conclusion and Outlook	32
Appendix A Multisite inhibition with different K_I values	36

Appendix B	Checking the results using MATLAB	38
B.1	Controller motif 2 without C and with exponential increase	38
B.2	Controller motif 2 with C and exponential increase	39
B.3	Controller motif 2 with C and first order autocatalysis and exponential increase	39
B.4	Controller motif 2 with C and second order autocatalysis	40
B.5	Oscillatory Controller motif 2 with exponential increase	40
B.6	Oscillatory Controller motif 2 with C and exponential increase	41
Appendix C	Fortran and MATLAB program parts	42

List of Figures

1.1	Controller motifs based on the with positive and negative feedback loops. A is a controlled variable and E is a the controller species. The dashed lines show how and which process does the A or E control or influence.	3
1.3	Integral control in the negative feedback scheme. The difference between set point of variable A and an actual value of A is integrated over time and then fed back in the process that generates variable A. This ensures that the variable is at the given set point	4
1.2	The eight basic controller motifs divided in the two classes: inflow controllers and outflow controllers.	4
1.4	General structure of motif 2 inflow controller based on depression kinetics.	5
1.5	Example of the controller breakdown. Controller is not able to keep the controlled variable A at a set point and it breaks down as the perturbation increases. The point of breakdown is shown with arrow.	6
1.6	Reversible noncompetitive inhibition. Both inhibitor and the substrate can bind to the enzyme on different binding sites. Although the substrate binds to the enzyme the enzymatic reaction does not proceed while inhibitor is bound.	7
1.7	Reversible noncompetitive multisite inhibition. Substrate can bind to more binding sites on the enzyme independent of the binding of inhibitor.	8
1.8	The oscillatory behaviour of the controller motif 2. It illustrates the ability of the controller to maintain homeostasis by having the oscillatory behaviour. As the perturbation k_2 is increased from 1.0 to 2.0 the average $\langle A \rangle$ of is maintained at the set point of 2. Frequency of the controller is increased. Still average value of $\langle E \rangle$ is decreasing and the controller reaches breakdown upon any further increase in k_2	10
1.9	The breakdown of the controller motif 2 with oscillatory behaviour. Controller is able to keep the A at A_{set} when the increase in perturbation is low but when it gets high ($k_1 = 200.0$) the controller is not able to keep the homeostasis and it breaks down.	10
4.1	The effect of different inhibition constants on the controller motif 2 when the k_1 increases exponentially as shown on the Figure 4.2 right panel. In the phase 1 the controller is at a steady state. In the phase 2 the k_1 starts to increase exponentially and the different behaviour of the controller E is observed. The E_1 and A_1 are values when $K_I=10$, E_2 and A_2 when $K_I=1$, E_3 and A_3 when $K_I=0.1$, and E_4 and A_4 when $K_I=1 \times 10^{-3}$. The other rate constants are: $k_2(\text{max compensatory rate})=1 \times 10^5$, $k_3=5 \times 10^3$, $k_4=1 \times 10^3$, $K_M=1 \times 10^{-6}$. Initial concentrations: $A=5.0$ (for all K_I values), $E_1=1 \times 10^5$, $E_2=1 \times 10^4$, $E_3=1 \times 10^3$, $E_4=10$	14

4.2	The effect of multisite inhibition on the controller motif 2 when the k_1 increases exponentially. In the phase 1 the controller is at a steady state. In the phase 2 the k_1 starts to increase exponentially and the different responses are observed for different numbers of binding sites n . Rate constants are: $K_I=0.1$, k_2 (max compensatory rate)= 1×10^5 , $k_3=5 \times 10^3$, $k_4=1 \times 10^3$, $K_M=1 \times 10^{-6}$. Initial concentrations: $A=5.0$ (for all n), E ($n=2$) = 9.9 , E ($n=4$)= 0.9	15
4.3	Controller motif 2 with additional variable C which is dependant on the concentration of E	16
4.4	Controller motif 2 with variable C which is dependant on the concentration of E illustrated on the Figure 4.4. Left panel: Concentrations of A and E as a function of time with different k_5/k_6 rate constants. Blue curves A_3 and E_3 correspond to the calculations without C (Figure 4.2 with $n=4$). Right panel: Concentrations of C with different k_5/k_6 rate constants as a function of time. Phase 1: the controller is at steady state at its set-point $A_{set}=5.0$ at constant $k_1=2.0$. Phase 2: k_1 increases exponentially according to the inset in the left panel of Figure 4.2. k_5 and k_6 values and initial concentrations for the different A_i , E_i , C_i curves: $i=1$, $k_5=10.0$, $k_6=0.01$, $A_0=5.0$, $E_0=2.412$, $C_0=39.81$; $i=2$, $k_5=1.0$, $k_6=0.1$, $A_0=5.0$, $E_0=0.9$, $C_0=1.0$; $i=3$, no C (Figure 4.2) with $n=4$; $i=4$, $k_5=k_6=0.1$, $A_0=5.0$, $E_0=0.531$, $C_0=0.158$. Other rate constant values: $k_2=1 \times 10^5$, $k_3=5 \times 10^3$, $k_4=1 \times 10^3$, $K_M=1 \times 10^{-6}$, $K_I=0.1$	17
4.5	Controller motif 2 with autocatalytic generation of C	18
4.6	Controller motif 2 with first order autocatalytic generation of C and linear increase in k_1 . Left panel: Concentrations of A and E as a function of time while perturbation increases linearly. Phase one is 100(au) and $k_1=2$ the controller is able to keep the A at the steady state. In the phase 2 at the time 100(au) the perturbation starts to increase linearly by the Equation 4.8. The controller is able to keep the A at the A_{set} , E decreases in the concentration and it eventually reached the steady state. Other rate constants are: $K_I=10$, k_2 (max compensatory rate)= 1×10^5 , $k_3=5 \times 10^3$, $k_4=1 \times 10^3$, $K_M=1 \times 10^{-6}$. Initial concentrations: $A=5.0$, $E=8.2 \times 10^3$, $C=2.3 \times 10^{13}$	20
4.7	Controller motif 2 with first order autocatalytic generation of C and step wise increase in k_1 . Left panel: Concentrations of A and E as a function of time while perturbation increases step wise. Phase one is 10(au) and $k_1=2$. The phase 2 is 100 (au) and $k_1=10$. The phase 3 is 100 (au) $k_1=20$. Other rate constants are: $K_I=10$, k_2 (max compensatory rate)= 1×10^5 , $k_3=5 \times 10^3$, $k_4=1 \times 10^3$, $K_M=1 \times 10^{-6}$. Initial concentrations: $A=5.0$, $E=2.5 \times 10^3$, $C=4.4 \times 10^1$	20
4.8	Controller motif 2 with first order autocatalytic generation of C and exponential increase in k_1 . Left panel: Concentrations of A and E as a function of time while perturbation increases exponentially in the phase 2. In the phase which is 10(au) long and $k_1=2$ the controller is able to keep the A at the steady state. In the phase 2 at the time 10(au) the perturbation starts to increase exponentially by the Equation 4.9. The controller keeps the A at the A_{set} while the E increases in concentration. Other rate constants are: $K_I=10$, $k_2=1 \times 10^5$, $k_3=5 \times 10^2$, $k_4=1 \times 10^2$, $k_5=10.0$, and $k_6=1.0$. $K_M=1 \times 10^{-6}$, $K_I=0.1$, $n=4$ (Equation 4.2).	21

- 4.9 Controller motif 2 with first order autocatalytic generation of C and hyperbolic increase in k_1 . Left panel: Concentrations of A and E as a function of time while perturbation increases hyperbolic in the phase 2. In the phase 1 which lasts one time unit (not shown) the controller is at its set point $A_{set} = 5.0$ and the $k_1=2.0$. In the phase 2 k_1 increases hyperbolic by the Equation 4.10, where $K_I=0.1$, $k_2=1 \times 10^5$, $k_3=5 \times 10^2$, $k_4=1 \times 10^2$, $k_5=10.0$, and $k_6=1.0$. $K_M=1 \times 10^{-6}$, $n = 4$ (Equation 4.2). The right panel shows the concentrations of k_1 and C as function of time in the short moment before they reach infinity limit. 21
- 4.10 Controller motif 2 with second order autocatalytic generation of C and linear increase in k_1 . Left panel: Concentrations of A and E as a function of time while perturbation increases linearly in the phase 2. In the phase 1 which lasts one time unit the controller is at its set point $A_{set} = 5.0$ and the constant $k_1=2.0$. In the phase 2 k_1 increases linearly by the Equation 4.9, where $K_I=0.1$, $k_2=1 \times 10^5$, $k_3=5 \times 10^2$, $k_4=1 \times 10^2$, $k_5=10.0$, and $k_6=1.0$. $K_M=1 \times 10^{-6}$, $n = 4$ (Equation 4.2). Initial concentrations are: $A_0 = 5.0, E_0 = 0.9$ and $C_0 = 1.0$ The right panel shows the concentrations of k_1 and C as function of time. 22
- 4.11 Controller motif 2 with second order autocatalytic generation of C and step wise increase in k_1 . Left panel: Concentrations of A and E as a function of time while perturbation increases step wise in the phase 2 and phase 3. All phases are 10 time units long and at the end of each phase the A is at $A_{set} = 5.0$. Other concentrations are $K_I=0.1$, $k_2=1 \times 10^5$, $k_3=5 \times 10^2$, $k_4=1 \times 10^2$, $k_5=10.0$, and $k_6=1.0$. $K_M=1 \times 10^{-6}$, $n = 4$ (Equation 4.2). Initial concentrations are: $A_0 = 5.0, E_0 = 0.9$ and $C_0 = 1.0$ The right panel shows the concentrations of k_1 and C as function of time. 22
- 4.12 Controller motif 2 with second order autocatalytic generation of C and exponential increase in k_1 . Left panel: Concentrations of A and E as a function of time while perturbation increases exponentially in the phase 2. In the phase 1 which lasts one time unit the controller is at its set point $A_{set} = 5.0$ and the constant $k_1=2.0$. In the phase 2 k_1 increases exponentially by the Eq 4.9, where $K_I=0.1$, $k_2=1 \times 10^5$, $k_3=5 \times 10^2$, $k_4=1 \times 10^2$, $k_5=10.0$, and $k_6=1.0$. $K_M=1 \times 10^{-6}$, $n = 4$ (Equation 4.2). Initial concentrations are: $A_0 = 5.0, E_0 = 0.9$ and $C_0 = 1.0$ The right panel shows the concentrations of k_1 and C as function of time. 23
- 4.13 Controller performance with second-order autocatalysis in C (Equation 4.7) and hyperbolic increase of k_1 (Equation 4.10). Phase 1 (not shown): the controller is at steady state at its set-point $A_{set}=5.0$ with constant $k_1=2.0$. Phase 1 lasts 1 time unit. Initial concentrations: $A_0=5.0$, $E_0=0.9$, $C_0=1.0$. Phase 2: k_1 increases hyperbolic. Rate constant values: $k_2=1 \times 10^5$, $k_3=5 \times 10^2$, $k_4=1 \times 10^2$, $k_5=10.0$, and $k_6=1.0$. $K_M=1 \times 10^{-6}$, $K_I=0.1$, $n = 4$ (Equation 4.2). Right panel: k_1 and C as a function of time just before k_1 reaches the infinity limit. At time 21.249997 $k_1=1.4 \times 10^7$, $C=5.4 \times 10^6$. Left panel: corresponding A and E concentrations as a function of time. 24

- 4.14 Breakdown of the controller motif 2 when perturbation increases stepwise (panel a). In panel b the controller does not break down. The breakdown is stopped by increasing the k_2 value from $k_2=6$ in the first two phases to the to the $k_2=1 \times 10^6$ in the third phase (panel b). Initial concentrations used are: $A_0=5.2$, $E_0=6.9$ and other rate constants are the same in all three phases and as follows: $k_3=5 \times 10^2$, $k_4=1 \times 10^2$, $k_5=50.0$, and $k_6=1.0$. $K_M=1 \times 10^{-6}$, $K_I=0.1$. The k_1 increases from $k_1=1.0$ in phase 1 to the $k_1=3.0$ in phase 2 and further to the $k_1=10.0$ in the phase 3 (panel c). 26
- 4.15 Controller motif 2 with step wise increase in k_1 an multisite inhibition $n=4$. Left panel: Concentrations of A and E as a function of time while perturbation increases step wise and average concentrations of $\langle A \rangle$ and $\langle E \rangle$. All phases are 50 time units long and the k_1 in three phases are: In phase 1: $k_1=1$; In phase 2: $k_1=3$; In phase 3: $k_1 = 10$ Other concentrations are $K_I=0.1$, $k_2=6$, $k_3=5 \times 10^1$, $k_4=1 \times 10^1$, $K_M=1 \times 10^{-6}$, $n = 4$. Initial concentrations are: $A_0 = 5.5, E_0 = 3.1$. The right panel shows the concentration of k_1 as function of time. 27
- 4.16 Controller motif 2 with linear increase in k_1 by Equation 4.8 and multisite inhibition $n=4$. Left panel: Concentrations of A and E as a function of time while perturbation increases linear and average concentrations of $\langle A \rangle$ and $\langle E \rangle$. In the first phase which is 20 time units long the $k_1=5$ and after that is increases linearly in the phase 2 which is 50 time units long. Other concentrations are $K_I=1$, $k_2=1 \times 10^5$, $k_3=5 \times 10^1$, $k_4=1 \times 10^1$, $K_M=1 \times 10^{-6}$, $n = 4$. Initial concentrations are: $A_0 = 1.5, E_0 = 2.1$. The right panel shows the concentration of k_1 as function of time. 27
- 4.17 Controller motif 2 with exponential increase in k_1 by Equation 4.9 and multisite inhibition $n=4$. Left panel: Concentrations of A and E as a function of time while perturbation increases linear and average concentrations of $\langle A \rangle$ and $\langle E \rangle$. In the first phase which is 20 time units long the $k_1=5$ and after that is increases linearly in the phase 2 which is 50 time units long. Other concentrations are $K_I=1$, $k_2=1 \times 10^5$, $k_3=5 \times 10^1$, $k_4=1 \times 10^1$, $K_M=1 \times 10^{-6}$, $n = 4$. Initial concentrations are: $A_0 = 1.5, E_0 = 2.1$. The right panel shows the concentration of k_1 as function of time. 28
- 4.18 Controller motif 2 with hyperbolic increase in k_1 by Equation 4.10 and multisite inhibition $n=4$. Left panel: Concentrations of A and E as a function of time while perturbation increases linear and average concentrations of $\langle A \rangle$ and $\langle E \rangle$. In the first phase which is 10 time units long the $k_1=5$ and after that is increases hyperbolic until the infinity limit is reached in phase 2 at total time : 18.01. Other concentrations are $K_I=1$, $k_2=1 \times 10^5$, $k_3=5 \times 10^1$, $k_4=1 \times 10^1$, $K_M=1 \times 10^{-6}$, $n = 4$. Initial concentrations are: $A_0 = 1.5, E_0 = 2.1$. The right panel shows the concentration of k_1 as function of time. 28
- 4.19 Controller motif 2 with C , linear increase in k_1 by Equation 4.8 and multisite inhibition $n=4$. Left panel: Concentrations of A and E as a function of time while perturbation increases linearly and average concentrations of $\langle A \rangle$ and $\langle E \rangle$. In the first phase which is 20 time units long the k_1 is constant $k_1=2 = 0$ and then it starts to increase linearly by Equation 4.8 in the phase 2 which is 30 time units long. Other concentrations are $K_I=0.1$, $k_2=1 \times 10^5$, $k_3=5 \times 10^2$, $k_4=1 \times 10^2$, $K_M=1 \times 10^{-6}$, $n = 4$. Initial concentrations are: $A_0 = 5.2, E_0 = 6.9, C_0 = 1.8 \times 10^{-3}$. The right panel shows the concentration of k_1 and C as function of time. 29

4.20	Controller motif 2 with C , stepwise increase in k_1 and multisite inhibition $n=4$. All phases are 10 time units long and the k_1 in three phases are: In phase 1: $k_1 = 5$; In phase 2: $k_1 = 10$; In phase 3: $k_1 = 200$. Left panel: Concentrations of A and E as a function of time while perturbation increases stepwise and average concentrations of $\langle A \rangle$ and $\langle E \rangle$. Other concentrations are $K_I=0.1$, $k_2=1 \times 10^5$, $k_3=5 \times 10^2$, $k_4=1 \times 10^2$, $K_M=1 \times 10^{-6}$, $n = 4$. Initial concentrations are: $A_0 = 5.2, E_0 = 6.9, C_0 = 1.8 \times 10^{-3}$. The right panel shows the concentration of k_1 and C as function of time.	30
4.21	Controller motif 2 with C , exponential increase in k_1 by Equation 4.9 and multisite inhibition $n=4$. Left panel: Concentrations of A and E as a function of time while perturbation increases linear and average concentrations of $\langle A \rangle$ and $\langle E \rangle$. In the first phase which is 20 time units long the $k_1 = 2$ and after that is increases exponentially in the phase 2 which is 30 time units long. Other concentrations are $K_I=0.1$, $k_2=1 \times 10^5$, $k_3=5 \times 10^2$, $k_4=1 \times 10^2$, $K_M=1 \times 10^{-6}$, $n = 4$. Initial concentrations are: $A_0 = 5.2, E_0 = 6.9$ and $C_0 = 1.8 \times 10^{-3}$. The right panel shows the concentrations of k_1 and C as function of time.	31
4.22	Controller motif 2 with C , hyperbolic increase in k_1 by Equation 4.10 and multisite inhibition $n=4$. Left panel: Concentrations of A and E as a function of time while perturbation increases hyperbolic and average concentrations of $\langle A \rangle$ and $\langle E \rangle$. In the first phase which is 20 time units long the $k_1 = 2$ and after that is increases hypwerbolic in the phase 2 until the infinity limit is reached at time=40.24939. Other concentrations are $K_I=0.1$, $k_2=1 \times 10^5$, $k_3=5 \times 10^2$, $k_4=1 \times 10^2$, $K_M=1 \times 10^{-6}$, $n = 4$. Initial concentrations are: $A_0 = 5.2, E_0 = 6.9$ and $C_0 = 1.8 \times 10^{-3}$. The right panel shows the concentrations of k_1 and C as function of time.	31
A.1	Testing the multisite inhibition with $K_I=1 \times 10^{-3}$, n is the number of inhibition sites tested. E_1 and A_1 are for $n=1$, E_2 and A_2 are for $n=2$, E_4 and A_4 are for $n=4$. k_1 increases exponentially in the phase 2, $k_2=1 \times 10^5$, $k_3=5 \times 10^3$, $k_4=1 \times 10^3$	37
B.1	Comparing the results presented on the Figure 4.2 using MATLAB. The $n=4$ and all concentrations are as described under the Figure.	38
B.2	Comparing the results presented on the Figure 4.4 using MATLAB. Given result is comparing the result when $k_5=1.0$ and $k_5=0.1$. Other rate constants are the same as on the Figure we are comparing it to. Here on the right panel we have the C value for the controller as well as we show that the k_1 is increasing exponentially.	39
B.3	Comparing the results presented on the Figure 4.8 using MATLAB. All initial values and the rate constants are the same as in the Figure 4.8 . . .	39
B.4	Comparing the results presented on the Figure 4.12 using MATLAB. All initial values and the rate constants are the same as in the Figure 4.12 . .	40
B.5	Comparing the results presented on the Figure 4.17 using MATLAB. All initial values and the rate constants are the same as in the Figure 4.17. .	40
B.6	Comparing the results presented on the Figure 4.21 using MATLAB. All initial values and the rate constants are the same as in the Figure 4.21. .	41

C.1	The selected part of the Fortran program used to obtain the result presented on the Figure 4.12. In the panel a of the Figure we can see the LSODE loop of the program which here defines the perturbation. The highlighted is the Equation 4.9 used to calculate k_1 in the case of exponential increase. In the panel b of the Figure we can see all the rate equations used in this case.	43
C.2	The selected part of the MATLAB program used to obtain the result presented on the Figure B.4. In the panel a of the Figure we can see the assignments given for the program together with the Equations for calculations of concentrations of A, E and C . In the panel b of the Figure we can see all the rate constants, and numerical integration's used in this case.	44

*To the University of Stavanger in hope of better understanding and
more appreciation of computational biology . . .*

Chapter 1

Introduction

All single cell and multicellular organisms have an internal environment that is separated from outside environment with a membrane and the composition of this environment is controlled. They are as well able to receive and send information to other cells. Mechanisms by which the cells receive information and respond to changes in their environment is something that is part of the field called *cybernetics*. Cybernetics is introduced by Norbert Wiener [1] and it combines the biological and physiological term homeostasis with the mechanical theory. It connects the machines and living organisms.

1.1 Homeostasis

The homeostasis history goes all the way to the 18-th century when Claude Bernard introduced the term “milieu intérieur” or “internal environment” [2]. Bernard looked first into the blood composition and temperature and noticed that internal temperature of endothermic organisms varies only slightly although the outside temperature changes a lot. So he said that internal environment of an organism is controlled by organism itself and is independent from the outer environment. He then generalized this idea and said that: ”All of the vital mechanisms, however varied they may be, have always one goal, to main uniformity of the conditions of the life in the internal environment” [3].

The term homeostasis is then first defined by Cannon [4] in 1929 as the organisms ability to maintain the internal variables of an organism at constant or near constant values [5]. In other words the homeostasis is organisms ability to adapt to changes in the environment.

There are different systems in the organism that are homeostatically regulated and some of those are [6]:

1. Concentration of nutrients, waste products and O₂ and CO₂.
2. Changes in pH.
3. Concentration of salts, electrolytes and nutrients.
4. Blood pressure and volume.
5. Body temperature.

Some of these problems were addressed by Cannon itself in 1929. Since then there has been a lot of research projects that have identified different compounds to be homeostatic regulated, and some of them include levels of hormones [7] and levels of transcription factors and related compounds [8]. There have been as well identified a lot of controller motifs in the nature and those are addressed in the Supplementary Material of the Ref. [9]

One way of studying homeostasis, which was used in this research, is using control engineering and mathematical modeling.

1.2 Regulation of Homeostasis

In general, if we have some kind of system (for example pool of water) and we want to keep the variable (water temperature) in the system at the given value. Then we are going to have a sensor (thermometer) that is going to measure the value of the variable (temperature) and if the variable value drops under or gets higher the sensor is going to send the information to effector or controller to work (to heat or heat less) to get the variable at the desired value. This kind of sequence followed to achieve homeostasis is called a feedback loop.

The ways organism achieve homeostasis can be explained mathematically by constructing the systems called controller motifs. The simplest control motif is constructed by two substances A and E and these two-component motifs serve as building blocks. A is called controlled variable and E is the controller species. There are different ways A and E can influence each other in order to achieve homeostasis. A and E can affect each others synthesis or degradation by activation or inhibition but only one of these, this gives together 16 different controller motifs as shown on the Figure 1.1. The half

of these controller motifs have an overall negative feedback and half have a positive feedback. Disturbances in the concentration of A are compensated by E which adjusts the compensatory flow.

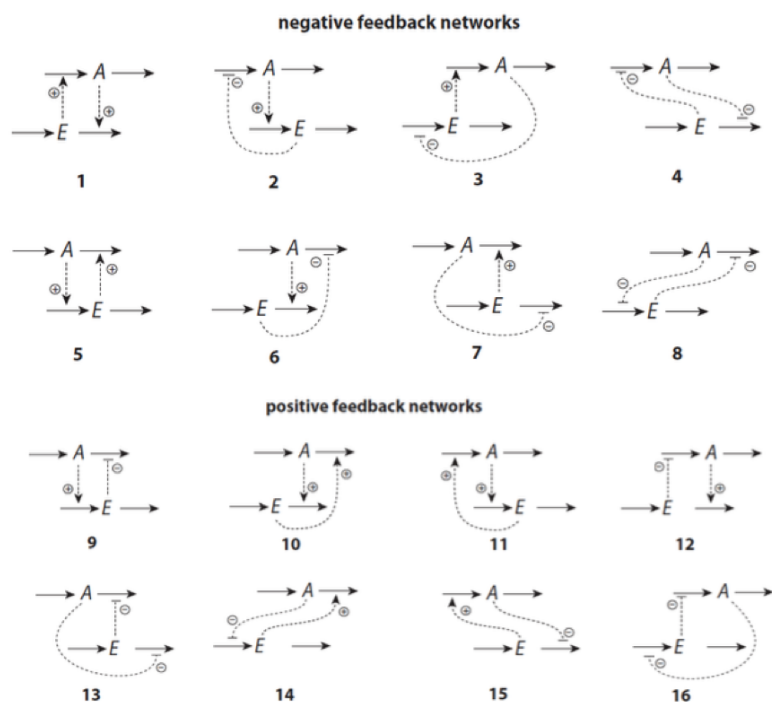


FIGURE 1.1: Controller motifs based on the with positive and negative feedback loops. A is a controlled variable and E is a the controller species. The dashed lines show how and which process does the A or E control or influence.

Most of known mechanisms are based on the negative feedback. In negative feedback the regulatory mechanism is activated only when the homeostasis is disturbed.

In the previous studies, as shown on Figure 1.2 there have been identified eight basic negative feedback loops also called controller motifs between controlled variable A and the controller variable E [9]. The controller motifs are divided in two groups *inflow controllers* and *outflow controllers*. In inflow controllers perturbation is causing the removal of controlled variable A from a system and controller work by adding more A to the system. In outflow controller controlled variable A is added to a system and outflow controller works by removing excess A from the system.

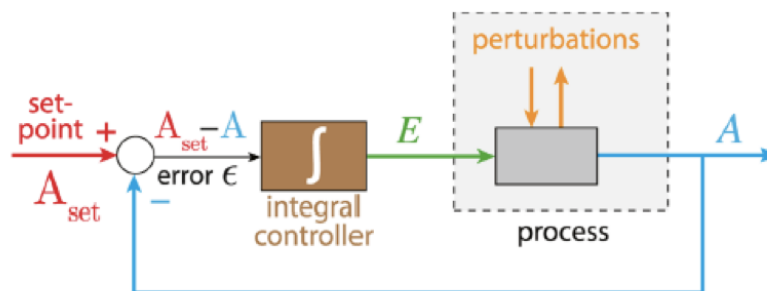


FIGURE 1.3: Integral control in the negative feedback scheme. The difference between set point of variable A and an actual value of A is integrated over time and then fed back in the process that generates variable A . This ensures that the variable is at the given set point

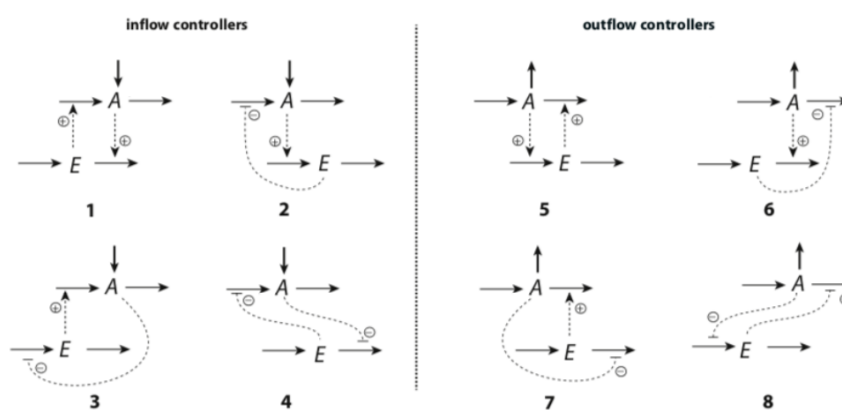


FIGURE 1.2: The eight basic controller motifs divided in the two classes: inflow controllers and outflow controllers.

In order to understand homeostasis scientists have tried to look into it from the engineer point of view and introduced control-engineering concept called *integral control*. Integral control is used in control engineering in order to keep variable at the desired, predetermined value, called set-point. This is done by the system that calculates the error (how much the value of a variable deviates from the set-point), integrates it and includes it back into the process of generation of the controlled variable as shown on Figure 1.3. This correction allows to bring the value of a variable precisely to the predetermined set-point.

It has been shown in previous studies that in order to achieve integral control certain kinetic conditions within negative feedback loop must be met. These include a zero-order degradation of controller E [9–12], autocatalytic formation of E [13–15] or second-order reaction [16, 17].

1.3 Controller motif 2

Eight controller motifs given in the Figure 1.2 have been tested with time-dependent perturbations [18] and the motif 2, inflow controller, based on the depression kinetics was able to work against the exponentially increasing perturbations as well as it can balance hyperbolic increase in perturbation with doubling times which decrease exponentially.

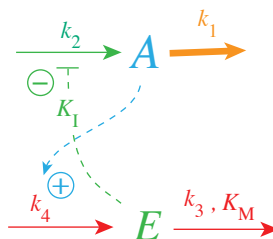


FIGURE 1.4: General structure of motif 2 inflow controller based on depression kinetics.

The scheme of the motif 2 is illustrated on the Figure 1.4 with the same color code as in the Figure 1.3. In the Figure 1.4, k_1 is the time dependent perturbation (removal of controlled variable from the system), k_2 is the compensatory flux which is inhibited by E , K_I is the inhibition constant, k_4 is the rate constant of zero order and A -induced synthesis of E . E is degraded by zero-order enzymatic reaction by the rate parameters $k_3(V_{max})$ and K_M .

The rate equations of the motif 2 controller are:

$$\dot{A} = \frac{k_2}{1 + \frac{E}{K_I}} - k_1 \cdot A \quad (1.1)$$

$$\dot{E} = k_4 \cdot A - \frac{k_3 \cdot E}{K_M + E} \quad (1.2)$$

where k_1 is the perturbation and $k_2/(1+(E/K_I))$ is the compensatory flux. To determine the set point we set the $\dot{E}=0$ and we solve for A_{ss} which gives us:

$$A_{ss} = A_{set} = \frac{k_3}{k_4} \quad (1.3)$$

This controller can be metaphorically compared to the plane which stands at start of the runway with engines in full thrust but it has the brakes on. Then when the brakes are released it starts moving and accelerating. What happens with the controller is that when the perturbation is increased the concentration of controller will decrease giving smaller inhibition constant K_I and this will lead to the increase in compensatory flux k_2 .

The maximum compensatory flux is reached when $E \leq K_I$ and all further increase in perturbation k_1 will lead to breakdown of the controller. Breakdown point happens when E is no longer able to compensate for the increased removal of A from the system. The point of breakdown, the value of k_1^{bd} when E can no longer compensate for the increased outflow, can be mathematically estimated by setting $E=K_I$ and solving for k_1 from the 1.1 with $\dot{A}=0$. This gives us:

$$\dot{A} = \frac{k_2 K_I}{2K_I} - k_1^{bd} A_{set} = 0 \quad (1.4)$$

Solving for k_1^{bd} gives us:

$$k_1^{bd} \approx \frac{k_2}{2A_{set}} \quad (1.5)$$

The example of the controller breakdown is illustrated on the Figure 1.5 where controller E breaks down and is barely able to get the controlled variable A to a set point when the system collapses. In this case the perturbation increases exponentially in the phase 2.

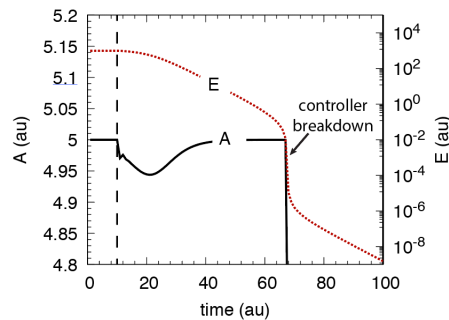


FIGURE 1.5: Example of the controller breakdown. Controller is not able to keep the controlled variable A at a set point and it breaks down as the perturbation increases. The point of breakdown is shown with arrow.

1.4 Effect of multisite inhibition

We can think of the controller motif 2 as a process of inhibition of an enzymatic process. The controller E in the controller motif 2 particularly, acts as an inhibitor that binds to the enzyme or transporter. It binds to the enzyme reversibly. The reversible inhibition means that the substrate and inhibitor can bind to an enzyme independently but the reaction can only proceed if inhibitor is not bound. The binding strength of an inhibitor is affected by the perturbation. The process is illustrated on the Figure 1.6.

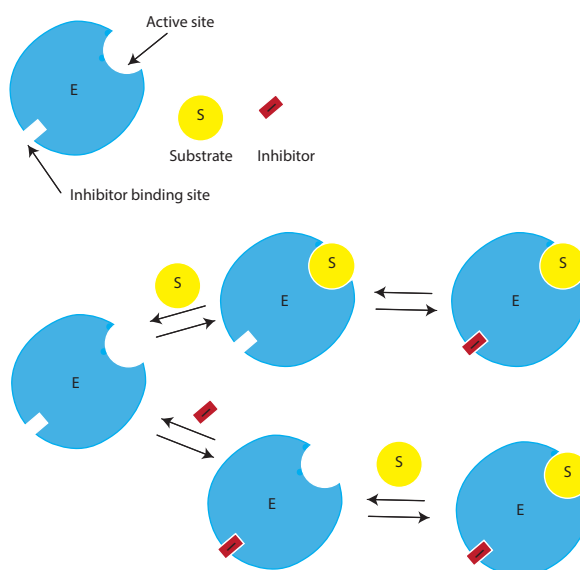


FIGURE 1.6: Reversible noncompetitive inhibition. Both inhibitor and the substrate can bind to the enzyme on different binding sites. Although the substrate binds to the enzyme the enzymatic reaction does not proceed while inhibitor is bound.

Inhibitors can have more than one binding site on the enzyme and this is called multisite inhibition and enzymes that have more binding sites are called *allosteric*. Multisite inhibition is illustrated on the Figure 1.7.

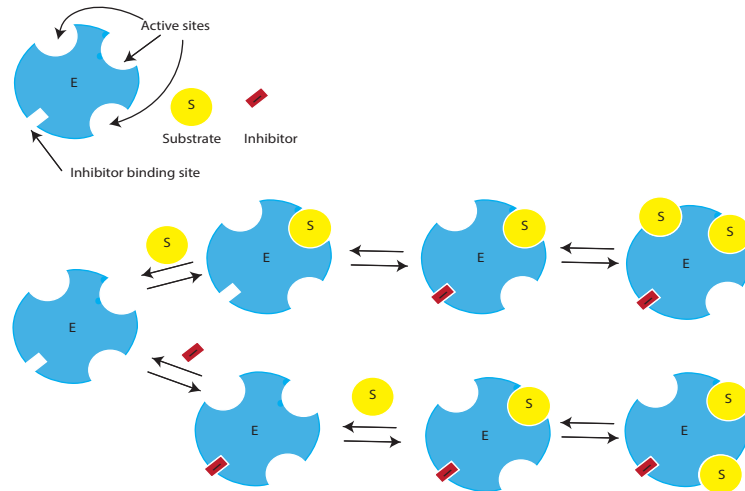


FIGURE 1.7: Reversible noncompetitive multisite inhibition. Substrate can bind to more binding sites on the enzyme independent of the binding of inhibitor.

In multisite inhibition the controller can bind to different binding sites with different binding constants. In theory the more binding sites a controller has, the controller will be more aggressive meaning that it will give faster response to the perturbation and get the controlled variable faster back at the steady state.

1.5 Oscillatory homeostasis

While the term oscillatory homeostasis can be seen as contradictory to the homeostasis as defined by Canon it is not necessarily like that. Oscillatory homeostasis is something that is not fully accepted by the control engineering because it is thought that systems are out of order when they oscillate and oscillations are thought to present the "breakdown of homeostasis" [19].

Many processes in biological systems are oscillatory [20–24] and even Cannon himself recognized that the normal level of glucose ranges between 70mg/dL and 130mg/dL and the values can oscillate [4] in the that range without compromising the system while any change that leads the concentration outside this range can lead to dysfunction and development of disease. This raises a question if oscillatory systems are in any case connected to the homeostatic systems.

It has previously been shown that the controller motif 2 shown on the Figure 1.4, can be modified to become oscillatory when degradation of A and E becomes zero-order with respect to A and E [25], in the case of step wise disturbances. This happens when $K_M \ll E$ and also $K_M \ll A$. The equations for A and E are then as follows:

$$\dot{A} = \frac{k_2}{1 + \frac{E}{K_I}} - k_1 \quad (1.6)$$

$$\dot{E} = k_2 A - k_3 \quad (1.7)$$

The controller is shown to be able to maintain the robust homeostasis in an average concentration $\langle A \rangle$ with

$$\langle A \rangle = \frac{1}{\tau} \int_0^\tau A(t) dt = A_{set} \quad (1.8)$$

This is shown on the Figure 1.8 taken from the previous research done on this subject [25].

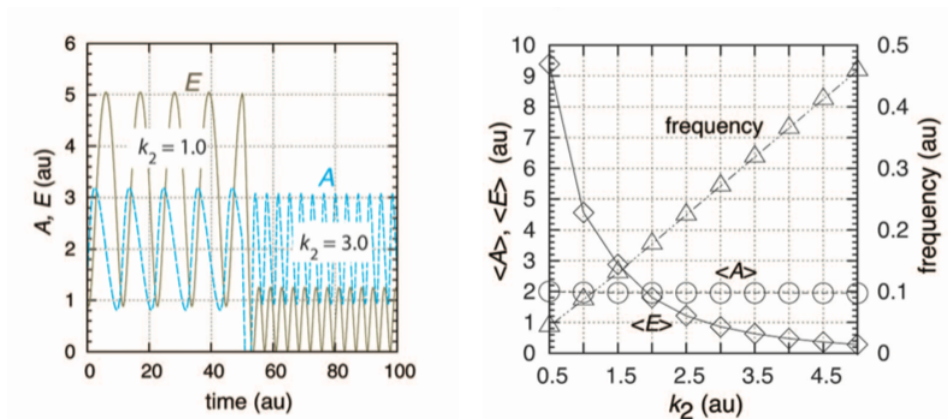


FIGURE 1.8: The oscillatory behaviour of the controller motif 2. It illustrates the ability of the controller to maintain homeostasis by having the oscillatory behaviour. As the perturbation k_2 is increased from 1.0 to 2.0 the average $\langle A \rangle$ of is maintained at the set point of 2. Frequency of the controller is increased. Still average value of $\langle E \rangle$ is decreasing and the controller reaches breakdown upon any further increase in k_2 .

This oscillatory controller however has the same challenge, it still breaks down when the increase in perturbation becomes too big and maximum compensatory flux is reached. This is shown on the Figure 1.9 where the perturbation increases step-wise and in the third phase the k_1 becomes too high and controller is no longer able to keep the A at the A_{set} .

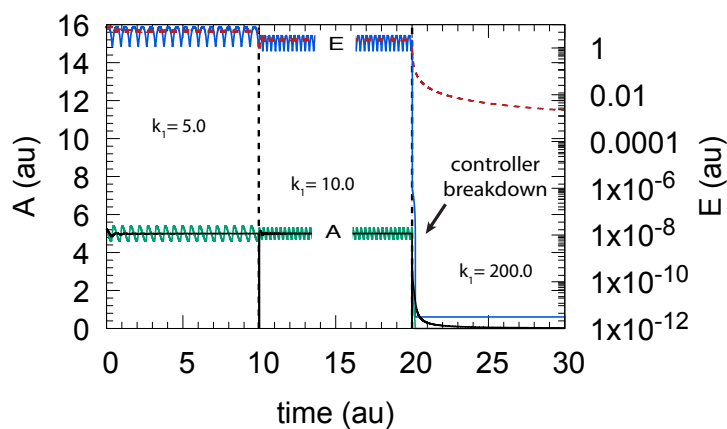


FIGURE 1.9: The breakdown of the controller motif 2 with oscillatory behaviour. Controller is able to keep the A at A_{set} when the increase in perturbation is low but when it gets high ($k_1 = 200.0$) the controller is not able to keep the homeostasis and it breaks down.

Chapter 2

Aim of thesis

The controller motif 2 is one controller motif based on depression that has been shown to be able to keep the variable at the set point even for rapidly increasing time-dependent perturbations placing this controller on the top of the list. However, this controller comes to the point of breakdown when $E \leq K_I$ and it can not keep the controlled variable A at a set point and all system collapses, homeostasis is not reached. This is illustrated on the Figure 1.5.

In this thesis we try to stop controller breakdown by implementing the multiisite inhibition and adding additional autocatalytic (positive feedback) loop while still keeping controllers main property - being based on the depression.

In addition, the controller is modified to become oscillatory as we inspect the homeostatic properties of such system.

Chapter 3

Methods

All calculations are done by using the Fortran subroutine LSODE. Part of the program and the important parameters that were varied to get the results including equations used can be seen in the Appendix. The plots were generated using Gnuplot (www.gnuplot.info) and annotated using Adobe Illustrator (www.adobe.com). Selected results were checked using MATLAB (mathworks.com). All concentrations of compounds are denoted by compounds names without square brackets and all are given in arbitrary units (a.u.). Time derivatives are written using "dot" notation.

Chapter 4

Results and Discussion

4.1 Influence of K_I on the controller performance

First point in testing the controller was to test the influence of the K_I - the inhibition constant of the controller on the controller lifetime. The controller tested is the one shown on the Figure 1.4 and the K_I is the constant by which E inhibits the synthesis of A . We wondered what happens if the strength of the inhibition is reduced. The values of K_I tested are $K_I=10$, $K_I=1$, $K_I=0.1$ and $K_I=1 \times 10^{-3}$. The k_1 is constant in the phase 1 when in the phase 2 at time $t_{p1}=10.0$ starts to increase exponentially as illustrated on the Figure 4.2 in the right panel. The results are shown on the Figure 4.1 where we observe that the changes in K_I at time does not prolong lifetime of the controller as breaks down at the same point.

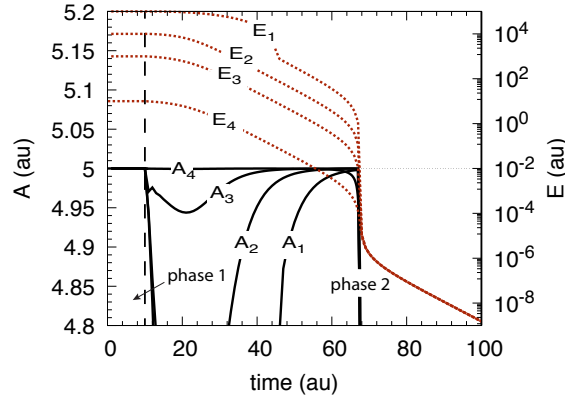


FIGURE 4.1: The effect of different inhibition constants on the controller motif 2 when the k_1 increases exponentially as shown on the Figure 4.2 right panel. In the phase 1 the controller is at a steady state. In the phase 2 the k_1 starts to increase exponentially and the different behaviour of the controller E is observed. The E_1 and A_1 are values when $K_I=10$, E_2 and A_2 when $K_I=1$, E_3 and A_3 when $K_I=0.1$, and E_4 and A_4 when $K_I=1 \times 10^{-3}$. The other rate constants are: k_2 (max compensatory rate) $=1 \times 10^5$, $k_3=5 \times 10^3$, $k_4=1 \times 10^3$, $K_M=1 \times 10^{-6}$. Initial concentrations: $A=5.0$ (for all K_I values), $E_1=1 \times 10^5$, $E_2=1 \times 10^4$, $E_3=1 \times 10^3$, $E_4=10$.

But, it is observed that controllers ability to keep A at A_{set} is increased with decreasing K_I value (compare for example A_1 when the $K_I=10$ with A_4 when $K_I=1 \times 10^{-3}$). It is obvious that the controller is more aggressive when the binding to the enzyme or transporter is not so strong. When we say "more aggressive" we think that controller is faster (it reacts faster to the perturbation) and more precise. This observation is easy to comprehend as we can think that the lower value of K_I gives weaker inhibition and in cases when perturbation happens and A is removed from the system, the weaker the inhibition the faster the response. Still in order to increase the lifetime of controller other approach must be made.

4.2 Implementation of multisite inhibition

We wondered what effect does the multiple binding sites of E to enzyme or transporter have on the controller efficiency. The controller motif 2 shown on Figure 4.3 is tested with the kind of inhibition shown on the Figure 1.7. The controller could bind to the different sites with different binding constants K_I but for the sake of simplicity we assume that all K_I values are the same, we have tested with the $K_I = 0.1$ We have tested behavior of the controller with one, two and four binding sites. The k_1 value, the perturbation has an exponential increase as shown on the right panel of Figure 4.2. The equation for calculating concentration of A for multisite inhibition used is Equation 4.2

$$\dot{A} = \frac{k_2}{1 + \left(\frac{E}{K_I}\right)^n} - k_1 \cdot A \quad (4.1)$$

where n is number of E molecules that bind to the enzyme or transporter (tested for $n=1,2$ and 4). The equation for \dot{E} is the Equation 4.3. The result can be seen on the Figure 4.2.

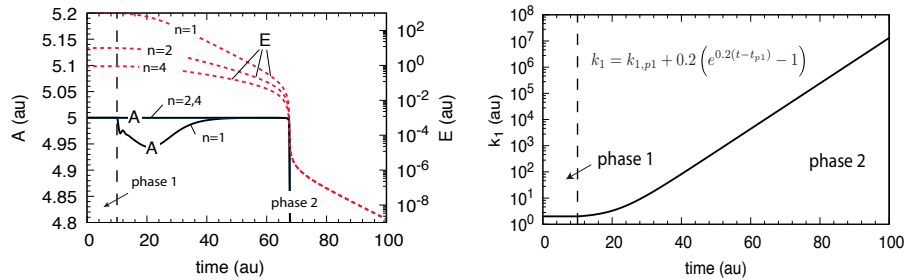


FIGURE 4.2: The effect of multisite inhibition on the controller motif 2 when the k_1 increases exponentially. In the phase 1 the controller is at a steady state. In the phase 2 the k_1 starts to increase exponentially and the different responses are observed for different numbers of binding sites n . Rate constants are: $K_I=0.1$, k_2 (max compensatory rate) $=1 \times 10^5$, $k_3=5 \times 10^3$, $k_4=1 \times 10^3$, $K_M=1 \times 10^{-6}$. Initial concentrations: $A=5.0$ (for all n), E ($n=2$) $=9.9$, E ($n=4$) $=0.9$.

The controller gets more aggressive and rapid with more binding sites. With 2 and more binding sites it is able to keep the controlled variable A at a set point $A_{set}=5$ even when k_1 starts to increase exponentially in the phase 2. The controller's lifetime is however not affected by the multisite inhibition, as the controller still breaks down at the same point.

We have tested the controller with $n=4$ binding sites with the $K_I=1 \times 10^{-3}$ which was shown to increase the aggressiveness in the first results (Figure 4.1). These results can be seen on the Figure A.1. We have chosen to continue with the $K_I=0.1$ because this value with $n=4$ binding sites gives the longest lifetime of the controller.

4.3 Increasing controller lifetime by increasing the maximum compensatory flux

As mentioned in the introduction the controller motif 2 has an issue because it breaks down when $E \leq K_I$ then maximum compensatory flux is reached and all further increase in perturbation k_1 will lead to breakdown of the controller. The Equation 4.5 indicates that the increasing maximum compensatory flux k_2 will lead to higher value of k_1^{bd} and with this increase in the controller lifetime. In order to increase the compensatory flux

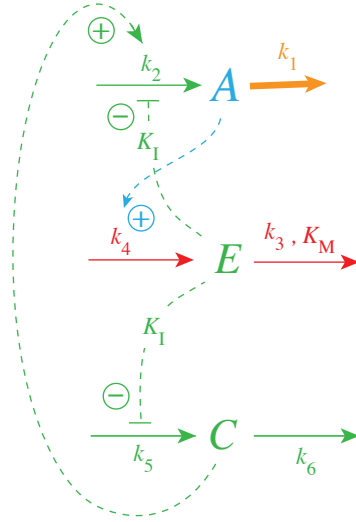


FIGURE 4.3: Controller motif 2 with additional variable C which is dependant on the concentration of E .

we have decided to add a new variable C . This variable is activated by the decrease in concentration of E and then it in turn works by increasing k_2 . This constructed controller motif is shown in Figure 4.3.

We assume that the E has only one binding site for the inhibition of generation of C . We also assume that the inhibition constant K_I is the same both for inhibition of generation of C and A . The equations for calculations are

$$\dot{A} = \frac{k_2 \cdot C}{1 + (\frac{E}{K_I})^n} - k_1 \cdot A \quad (4.2)$$

$$\dot{E} = k_4 \cdot A - \frac{k_3 \cdot E}{K_M + E} \quad (4.3)$$

$$\dot{C} = \frac{k_5}{1 - \frac{E}{K_I}} - k_6 \cdot C \quad (4.4)$$

Since we have shown that the controller is most aggressive and rapid when it has $n=4$ binding sites for the inhibition of generation of A as shown on the Figure 4.2 we use this further in our calculations. The controller is tested for exponential increase in k_1 as shown on the right panel of Figure 4.2. We have as well here varied ratios of rate constants for generation k_5 and decomposition k_6 of C to see the effect of this on the lifetime of the controller.

The results are presented on the Figure 4.4 and we observe that controller lifetime increase with the presence of C when the ratio of k_5/k_6 is high i.e. the rate of generation

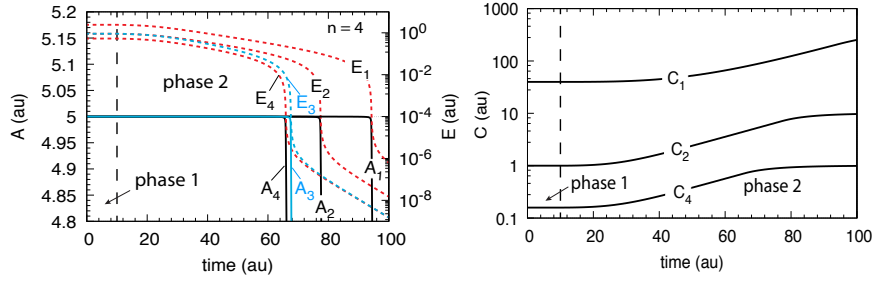


FIGURE 4.4: Controller motif 2 with variable C which is dependant on the concentration of E illustrated on the Figure 4.4. Left panel: Concentrations of A and E as a function of time with different k_5/k_6 rate constants. Blue curves A_3 and E_3 correspond to the calculations without C (Figure 4.2 with $n=4$). Right panel: Concentrations of C with different k_5/k_6 rate constants as a function of time. Phase 1: the controller is at steady state at its set-point $A_{set}=5.0$ at constant $k_1=2.0$. Phase 2: k_1 increases exponentially according to the inset in the left panel of Figure 4.2. k_5 and k_6 values and initial concentrations for the different A_i , E_i , C_i curves: $i=1$, $k_5=10.0$, $k_6=0.01$, $A_0=5.0$, $E_0=2.412$, $C_0=39.81$; $i=2$, $k_5=1.0$, $k_6=0.1$, $A_0=5.0$, $E_0=0.9$, $C_0=1.0$; $i=3$, no C (Figure 4.2) with $n=4$; $i=4$, $k_5=k_6=0.1$, $A_0=5.0$, $E_0=0.531$, $C_0=0.158$. Other rate constant values: $k_2=1 \times 10^5$, $k_3=5 \times 10^3$, $k_4=1 \times 10^3$, $K_M=1 \times 10^{-6}$, $K_I=0.1$.

is higher than the rate of decomposition of C . We have tested with the ratios of 1, 10 and 1000. For the sake of comparing we have plotted the result from the Figure 4.2 when $n=4$ and there is no variable C (blue lines in the Figure 4.4). The longest lifetime of the controller is achieved when rate constant for generation k_5 is much higher than the rate of decomposition for A_1/E_1 and A_2/E_2 while it is slightly lower than the controller without C when the ratio is between $k_5/k_6 = 1$. On the right panel of the Figure 4.4 we have shown the difference in C concentrations for different ratios and we observe the concentration of C is highest when ration of $k_5/k_6 = 1000$ and is increasing with increase in k_1 .

The lifetime of the controller is increased by this implementation but it still breaks down when value of E reaches the value of K_I . The point of breakdown can be estimated by solving the Equation 4.2 for k_1 , if we set $E=K_I$ and $\dot{A}=0$ we get

$$k_1^{bd} \approx \frac{k_2 C}{2A_{set}} \quad (4.5)$$

Since this controller still breaks down no further testing was preformed but we decide to introduce autocatalysis in C .

4.4 Implementing the positive feedback activation of C in order to stop the controller breakdown

In order to oppose the degradation of the E we decided to try to implement the positive feedback autocatalytic generation of C . Autocatalysis means that C is reactant in its own production, meaning it catalyzes its own generation. This however does not change the properties of the controller motif 2. Scheme of this motif can be seen on the Figure 4.5.

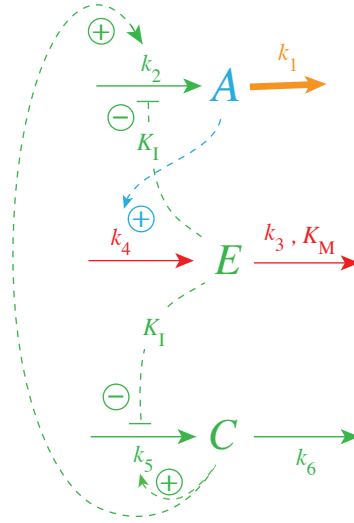


FIGURE 4.5: Controller motif 2 with autocatalytic generation of C .

The generation of C can be first and second order autocatalysis. The equation for the calculation of \dot{C} in first order autocatalysis is given by

$$\dot{C} = \frac{k_5 C}{1 - \frac{E}{K_I}} - k_6 * C \quad (4.6)$$

and for the second order autocatalysis

$$\dot{C} = \frac{k_5 C^2}{1 - \frac{E}{K_I}} - k_6 * C^2 \quad (4.7)$$

Other equations used are Equation 4.2 and Equation 4.3.

We have tested this controller motif by using the following assumptions that we found were increasing aggressiveness and lifetime of controller in the previous sections. We assume that E has $n=4$ binding sites on the enzyme or transporter involved in inhibition

of generation of A while it can bind to only one binding site for the inhibition of generation of C . The inhibition constants K_I have all the same values. Since this controller can have both first and second order autocatalysis in C we have tested both situations. To take the things one step further we have tested the controller for different types of perturbations. Until now we have tested different controller motifs only for exponential increase in perturbation but now we test the controller for exponential, hyperbolic, linear and step-wise increase in k_1 . The following equations are used for different increase in perturbations:

For linear increase in k_1

$$k_1 = k_{1,p1} + 1000(t - t_{p1}) \quad (4.8)$$

For exponential increase in k_1

$$k_1 = k_{1,p1} + 0.2(e^{0.2(t-t_{p1})} - 1) \quad (4.9)$$

For hyperbolic increase

$$k_1 = \frac{40.5}{\frac{40.5}{k_{1,p1}} - (t - t_{p1})} \quad (4.10)$$

4.4.1 First order autocatalysis in C

Implementation of first order autocatalysis in C using Equation 4.6 and testing it for different types of growth in perturbations. In the case of linear growth, the controller does not break down, it actually increases in concentration while A is kept at set point. This is shown on the Figure 4.6. In the right panel of this figure we see that the concentration of C increases as well as the perturbation increases.

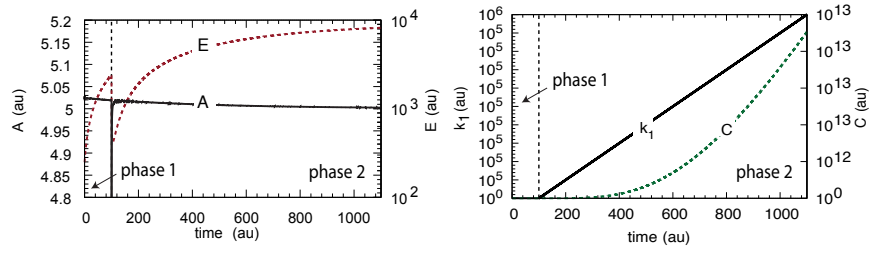


FIGURE 4.6: Controller motif 2 with first order autocatalytic generation of C and linear increase in k_1 . Left panel: Concentrations of A and E as a function of time while perturbation increases linearly. Phase one is 100(au) and $k_1=2$ the controller is able to keep the A at the steady state. In the phase 2 at the time 100(au) the perturbation starts to increase linearly by the Equation 4.8. The controller is able to keep the A at the A_{set} , E decreases in the concentration and it eventually reached the steady state. Other rate constants are: $K_I=10$, k_2 (max compensatory rate) $=1 \times 10^5$, $k_3=5 \times 10^3$, $k_4=1 \times 10^3$, $K_M=1 \times 10^{-6}$. Initial concentrations: $A=5.0$, $E=8.2 \times 10^3$, $C=2.3 \times 10^{13}$

We then test the controller with the step wise increase in k_1 with three phases. The result is shown in the Figure 4.7. We can see on the left panel of the Figure 4.7 that the controller will in the third phase be at the set point of $A_{set}=5.0$ from the start while it will need more time to reach the set point in the first two phases when k_1 is lower. So it is interesting to see that the controller takes actually more time to get to the set point when the perturbation is small while it is much faster when the perturbation is higher.

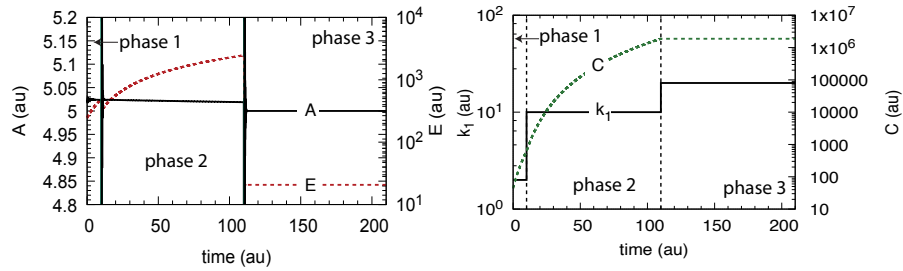


FIGURE 4.7: Controller motif 2 with first order autocatalytic generation of C and step wise increase in k_1 . Left panel: Concentrations of A and E as a function of time while perturbation increases step wise. Phase one is 10(au) and $k_1=2$. The phase 2 is 100 (au) and $k_1=10$. The phase 3 is 100 (au) $k_1=20$. Other rate constants are: $K_I=10$, k_2 (max compensatory rate) $=1 \times 10^5$, $k_3=5 \times 10^3$, $k_4=1 \times 10^3$, $K_M=1 \times 10^{-6}$. Initial concentrations: $A=5.0$, $E=2.5 \times 10^3$, $C=4.4 \times 10^1$

When we have exponential increase in the k_1 by the Equation 4.9 the A is kept at its set point $A_{set}=k_3/k_4=5.0$ and E does not break down but reaches a steady state as shown on the Figure 4.8. We observe also that value of C follows value of k_1 closely. The same situation is run using MATLAB, giving same results as shown in on Figure B.3 in B.3.

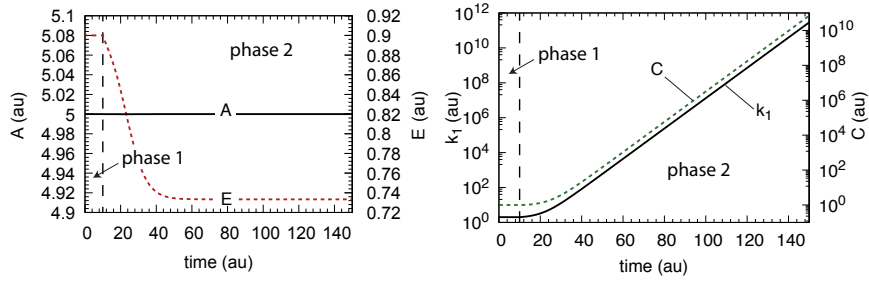


FIGURE 4.8: Controller motif 2 with first order autocatalytic generation of C and exponential increase in k_1 . Left panel: Concentrations of A and E as a function of time while perturbation increases exponentially in the phase 2. In the phase which is 10(au) long and $k_1=2$ the controller is able to keep the A at the steady state. In the phase 2 at the time 10(au) the perturbation starts to increase exponentially by the Equation 4.9. The controller keeps the A at the A_{set} while the E increases in concentration. Other rate constants are: $K_I=10$, $k_2=1 \times 10^5$, $k_3=5 \times 10^2$, $k_4=1 \times 10^2$, $k_5=10.0$, and $k_6=1.0$. $K_M=1 \times 10^{-6}$, $K_I=0.1$, $n = 4$ (Equation 4.2).

The most demanding task for the controller motif 2 with first order autocatalytic generation was to give the hyperbolic increase in perturbation. This type of perturbation is rapid and reaches infinity limit at certain time point. The k_1 increases hyperbolic by the Equation 4.10 where the k_1 is constant during the phase 1. Infinity limit is reached when time is $t = 20.25$. Although this is rapid increase in perturbation controller is still able to maintain the homeostasis all until the infinity limit when it breaks down as seen on the left panel on the Figure 4.9.

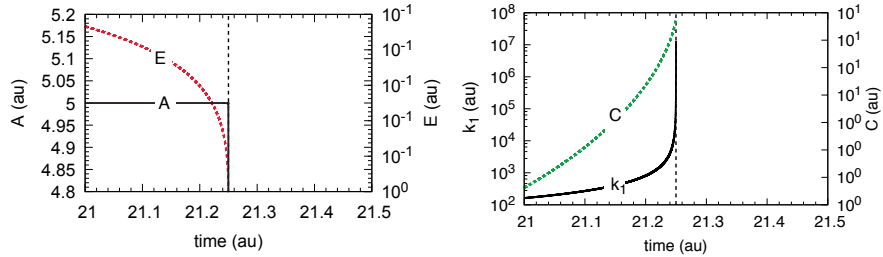


FIGURE 4.9: Controller motif 2 with first order autocatalytic generation of C and hyperbolic increase in k_1 . Left panel: Concentrations of A and E as a function of time while perturbation increases hyperbolic in the phase 2. In the phase 1 which lasts one time unit (not shown) the controller is at its set point $A_{set} = 5.0$ and the $k_1=2.0$. In the phase 2 k_1 increases hyperbolic by the Equation 4.10, where $K_I=0.1$, $k_2=1 \times 10^5$, $k_3=5 \times 10^2$, $k_4=1 \times 10^2$, $k_5=10.0$, and $k_6=1.0$. $K_M=1 \times 10^{-6}$, $n = 4$ (Equation 4.2). The right panel shows the concentrations of k_1 and C as function of time in the short moment before they reach infinity limit.

4.4.2 Second order autocatalysis in C

We test the controller shown on Figure 4.5 with the second order autocatalysis in C by Equation 4.7. First we test the linear increase in k_1 by the Eq 4.8. The result is shown on the Figure 4.10. The controller is now able to keep the A at the set point of 5 and it itself is in the steady state (left panel of the Figure 4.10). We observe also that the C follows the increase in the k_1 completely in the contrary of the linear increase with the first order autocatalysis shown on Figure 4.6 (right panel).

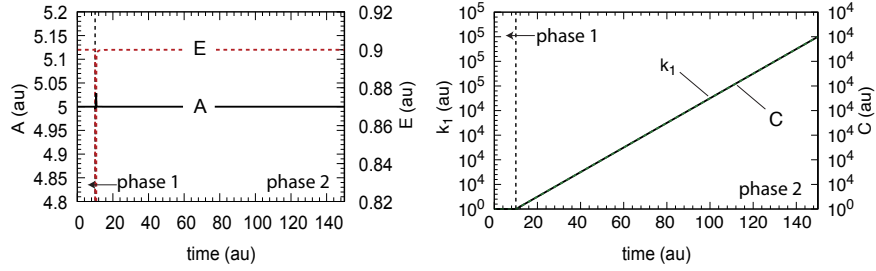


FIGURE 4.10: Controller motif 2 with second order autocatalytic generation of C and linear increase in k_1 . Left panel: Concentrations of A and E as a function of time while perturbation increases linearly in the phase 2. In the phase 1 which lasts one time unit the controller is at its set point $A_{set} = 5.0$ and the constant $k_1=2.0$. In the phase 2 k_1 increases linearly by the Equation 4.9, where $K_I=0.1$, $k_2=1 \times 10^5$, $k_3=5 \times 10^2$, $k_4=1 \times 10^2$, $k_5=10.0$, and $k_6=1.0$. $K_M=1 \times 10^{-6}$, $n = 4$ (Equation 4.2). Initial concentrations are: $A_0 = 5.0, E_0 = 0.9$ and $C_0 = 1.0$ The right panel shows the concentrations of k_1 and C as function of time.

When tested for the step wise increase in the k_1 the controller is able to keep the A at the set point in each phase. The result is shown on the Figure 4.11.

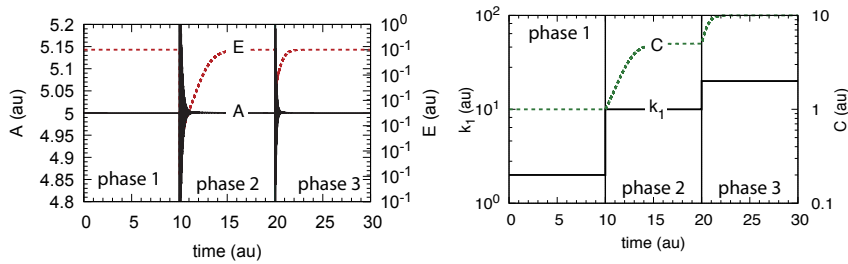


FIGURE 4.11: Controller motif 2 with second order autocatalytic generation of C and step wise increase in k_1 . Left panel: Concentrations of A and E as a function of time while perturbation increases step wise in the phase 2 and phase 3. All phases are 10 time units long and at the end of each phase the A is at $A_{set} = 5.0$. Other concentrations are $K_I=0.1$, $k_2=1 \times 10^5$, $k_3=5 \times 10^2$, $k_4=1 \times 10^2$, $k_5=10.0$, and $k_6=1.0$. $K_M=1 \times 10^{-6}$, $n = 4$ (Equation 4.2). Initial concentrations are: $A_0 = 5.0, E_0 = 0.9$ and $C_0 = 1.0$ The right panel shows the concentrations of k_1 and C as function of time.

In contrary to the first order autocatalysis shown on the Figure 4.7 where the controller needs more time to reach the set point the controller is at the set point in each phase. E itself is under homeostatic control and the set point can be calculated by setting Equation 4.7 to zero which leads to

$$E_{set} = K_I \left(\frac{k_5}{k_6} - 1 \right) \quad (4.11)$$

When we set in all values from the Figure 4.11 into the Equation 4.11 we get the value $E_{set} = 0.9$ which corresponds to the numerical value of E_{ss} and illustrated on the Figure 4.11 (left panel).

In the case of exponential increase and second order autocatalytic generation of C as shown on Figure 4.12 we do not observe to much difference when comparing to the Figure 4.8. Only thing that is observed is that E reaches $E_{set} = 0.9$ while E in 4.8 reaches steady state which is lower than the calculated E_{set} . The same situation is run using MATLAB, giving same results as shown in on Figure B.4 in B.4.

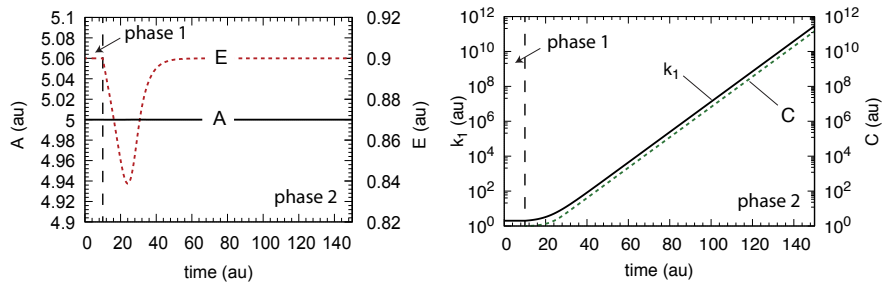


FIGURE 4.12: Controller motif 2 with second order autocatalytic generation of C and exponential increase in k_1 . Left panel: Concentrations of A and E as a function of time while perturbation increases exponentially in the phase 2. In the phase 1 which lasts one time unit the controller is at its set point $A_{set} = 5.0$ and the constant $k_1 = 2.0$. In the phase 2 k_1 increases exponentially by the Eq 4.9, where $K_I = 0.1$, $k_2 = 1 \times 10^5$, $k_3 = 5 \times 10^2$, $k_4 = 1 \times 10^2$, $k_5 = 10.0$, and $k_6 = 1.0$. $K_M = 1 \times 10^{-6}$, $n = 4$ (Equation 4.2). Initial concentrations are: $A_0 = 5.0, E_0 = 0.9$ and $C_0 = 1.0$. The right panel shows the concentrations of k_1 and C as function of time.

Further we test the same controller with the hyperbolic increase in perturbation. The result is shown on the Figure 4.13 where we can see that the controller is able to keep the A at a set point but the numerical value of E_{ss} is lower than calculated value of E_{set} which is 0.9. It is still able to keep E_{ss} before reaching the infinity limit which the controller with first order autocatalysis was not able to, recall the Figure 4.9. C is following the increase in the perturbation more closely (right panel of Figure 4.13) than in the case of first order autocatalysis (left panel of Figure 4.9).

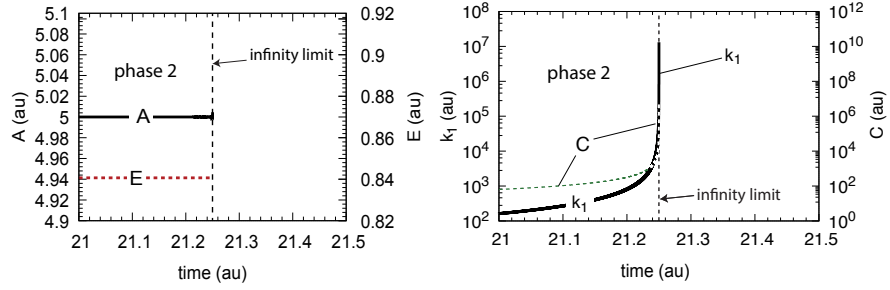


FIGURE 4.13: Controller performance with second-order autocatalysis in C (Equation 4.7) and hyperbolic increase of k_1 (Equation 4.10). Phase 1 (not shown): the controller is at steady state at its set-point $A_{set}=5.0$ with constant $k_1=2.0$. Phase 1 lasts 1 time unit. Initial concentrations: $A_0=5.0$, $E_0=0.9$, $C_0=1.0$. Phase 2: k_1 increases hyperbolic. Rate constant values: $k_2=1 \times 10^5$, $k_3=5 \times 10^2$, $k_4=1 \times 10^2$, $k_5=10.0$, and $k_6=1.0$. $K_M=1 \times 10^{-6}$, $K_I=0.1$, $n = 4$ (Equation 4.2). Right panel: k_1 and C as a function of time just before k_1 reaches the infinity limit. At time 21.249997 $k_1=1.4 \times 10^7$, $C=5.4 \times 10^6$. Left panel: corresponding A and E concentrations as a function of time.

4.5 Oscillatory homeostasis

As shown on the Figure 1.4 becomes oscillatory when degradation of A and E becomes zero-order with respect to A and E . It is observed that controller breaks down when k_1 is high and $K_M \ll E$ and $K_M \ll A$. The controller stops oscillating and can not keep the $A=A_{set}$ as shown on the panel a Figure 4.14 [25]. The equations are then Equation 1.6 for A and Equation 1.7 for E .

The breakdown problem could be solved by increasing the compensatory flux, the value of k_2 . The point of breakdown can be calculated from the Equation 1.6 if we set $E=K_I$ and $\dot{A}=0$ which gives us

$$k_1^{bd} \approx \frac{k_2}{2} \quad (4.12)$$

So we first try by adjusting the k_2 when the k_1 (perturbation) increases stepwise in the manner shown in the Figure 4.14 (panel c). We first observe that the controller breaks down when the $k_1=10.0$ (the panel a). But when we increase value of k_2 in just one order of magnitude the controller keeps oscillating and is able to keep the $\langle A \rangle$ at the A_{set} (panel b 4.14). In order to keep up with the increase in perturbation the concentration of E increases (see the third phase of the the panel b, Figure 4.14).

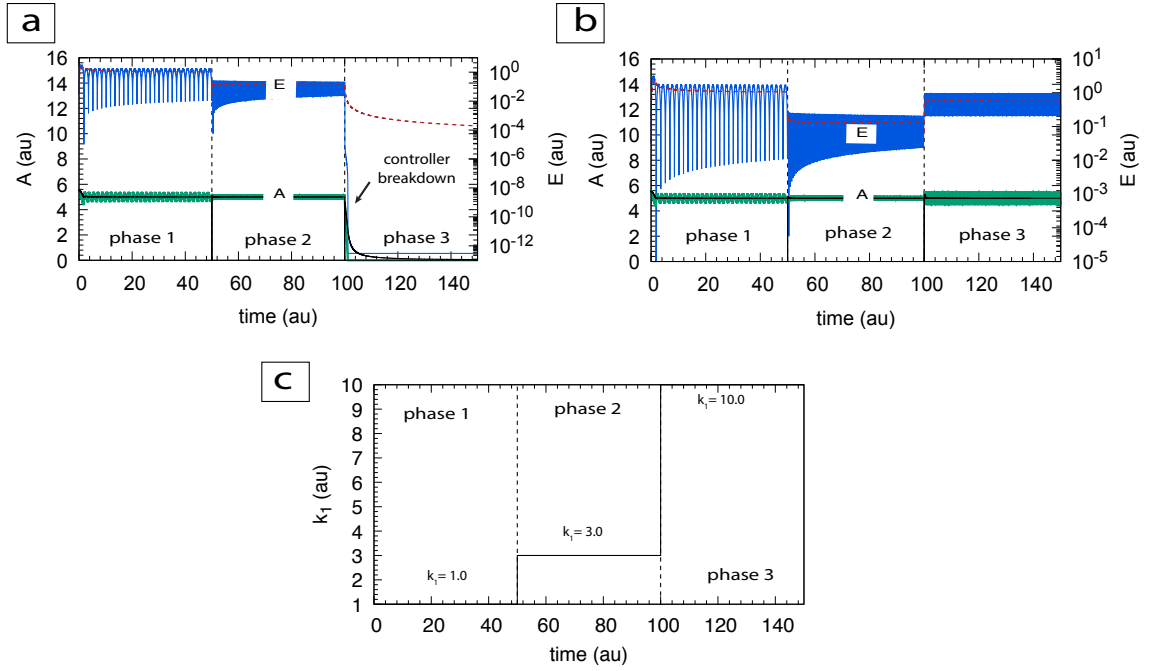


FIGURE 4.14: Breakdown of the controller motif 2 when perturbation increases stepwise (panel a). In panel b the controller does not break down. The breakdown is stopped by increasing the k_2 value from $k_2=6$ in the first two phases to the to the $k_2=1 \times 10^6$ in the third phase (panel b). Initial concentrations used are: $A_0=5.2$, $E_0=6.9$ and other rate constants are the same in all three phases and as follows: $k_3=5 \times 10^2$, $k_4=1 \times 10^2$, $k_5=50.0$, and $k_6=1.0$. $K_M=1 \times 10^{-6}$, $K_I=0.1$. The k_1 increases from $k_1=1.0$ in phase 1 to the $k_1=3.0$ in phase 2 and further to the $k_1=10.0$ in the phase 3 (panel c).

4.5.1 Time dependent perturbations for controller motif 2

Further we have decided to test the controller motif 2, Figure 1.4 for multisite inhibition, choosing four binding sites for E . In this case the Equations for calculating the \dot{E} is Equation 1.7 and for \dot{A} when there is $n=4$ binding sites is

$$\dot{A} = \frac{k_2}{1 + \left(\frac{E}{K_I}\right)^n} - k_1 \quad (4.13)$$

The controller is first tested for the stepwise perturbations. We observe that the A oscillates around the set point A_{set} . In the case of E it oscillates and concentration decreases in phase 2 compared to phase 1 while it increases in the third phase when $k_1=10$. The controller is able to keep the $\langle A \rangle$ at the A_{set} . The result is presented in the Figure 4.15.

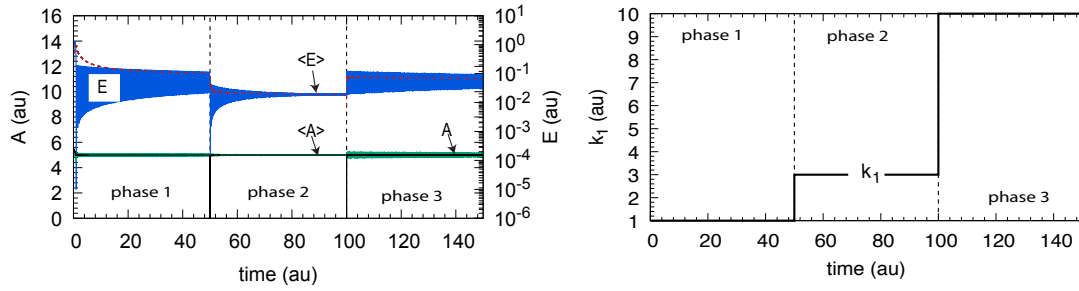


FIGURE 4.15: Controller motif 2 with step wise increase in k_1 an multisite inhibition $n=4$. Left panel: Concentrations of A and E as a function of time while perturbation increases step wise and average concentrations of $\langle A \rangle$ and $\langle E \rangle$. All phases are 50 time units long and the k_1 in three phases are: In phase 1: $k_1=1$; In phase 2: $k_1=3$; In phase 3: $k_1=10$ Other concentrations are $K_I=0.1$, $k_2=6$, $k_3=5 \times 10^1$, $k_4=1 \times 10^1$, $K_M=1 \times 10^{-6}$, $n=4$. Initial concentrations are: $A_0=5.5, E_0=3.1$. The right panel shows the concentration of k_1 as function of time.

The controller motif 2 is further tested for the linear, exponential and hyperbolic increase in k_1 when the cooperativity is $n=4$.

In case of linear increase the k_1 is increasing by the Equation 4.8. The k_1 is constant in the phase 1 and then it increases in the phase 2. The controlled variable A oscillates around the set point $A_{set}=5.0$. $\langle E \rangle$ reaches steady state in phase 2 when it decreases in the phase 2. The result is shown on the Figure 4.16.

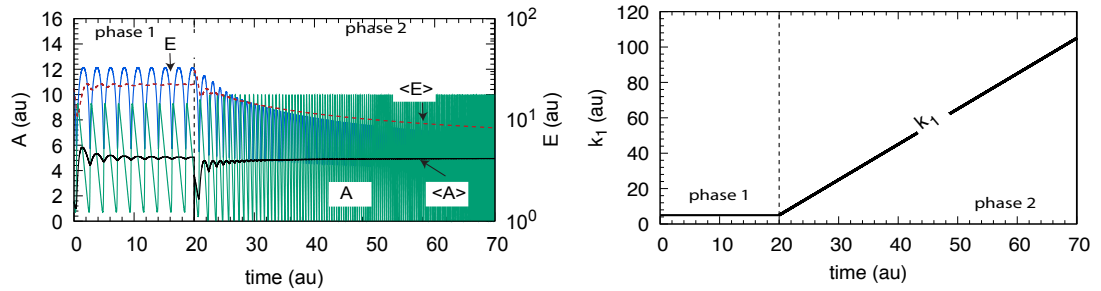


FIGURE 4.16: Controller motif 2 with linear increase in k_1 by Equation 4.8 and multisite inhibition $n=4$. Left panel: Concentrations of A and E as a function of time while perturbation increases linear and average concentrations of $\langle A \rangle$ and $\langle E \rangle$. In the first phase which is 20 time units long the $k_1=5$ and after that is increases linearly in the phase 2 which is 50 time units long. Other concentrations are $K_I=1$, $k_2=1 \times 10^5$, $k_3=5 \times 10^1$, $k_4=1 \times 10^1$, $K_M=1 \times 10^{-6}$, $n=4$. Initial concentrations are: $A_0=1.5, E_0=2.1$. The right panel shows the concentration of k_1 as function of time.

We have further tested the controller for the exponential increase in perturbation. The perturbation is increasing exponentially by Equation 4.9. The average value of the

controlled variable ($\langle A \rangle$) is again kept at the A_{set} . The result is shown on Figure 4.17. This result was compared using MATLAB and can be seen on the Figure B.5 in B.5.

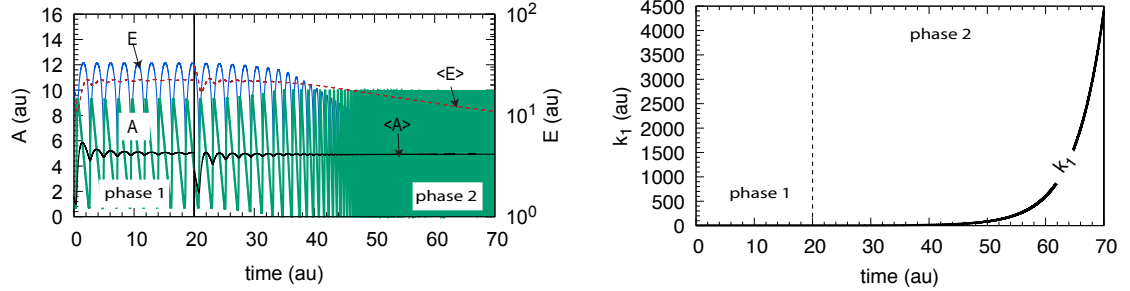


FIGURE 4.17: Controller motif 2 with exponential increase in k_1 by Equation 4.9 and multisite inhibition $n=4$. Left panel: Concentrations of A and E as a function of time while perturbation increases linear and average concentrations of $\langle A \rangle$ and $\langle E \rangle$. In the first phase which is 20 time units long the $k_1=5$ and after that is increases linearly in the phase 2 which is 50 time units long. Other concentrations are $K_I=1$, $k_2=1 \times 10^5$, $k_3=5 \times 10^1$, $k_4=1 \times 10^1$, $K_M=1 \times 10^{-6}$, $n = 4$. Initial concentrations are: $A_0 = 1.5, E_0 = 2.1$. The right panel shows the concentration of k_1 as function of time.

For the hyperbolic increase the k_1 is increasing hyperbolic in the phase 2 by the equation 4.10. The controller is able to keep the average value of A at the A_{set} until the infinity limit is reached and controller breaks down. This is shown on the Figure 4.18.

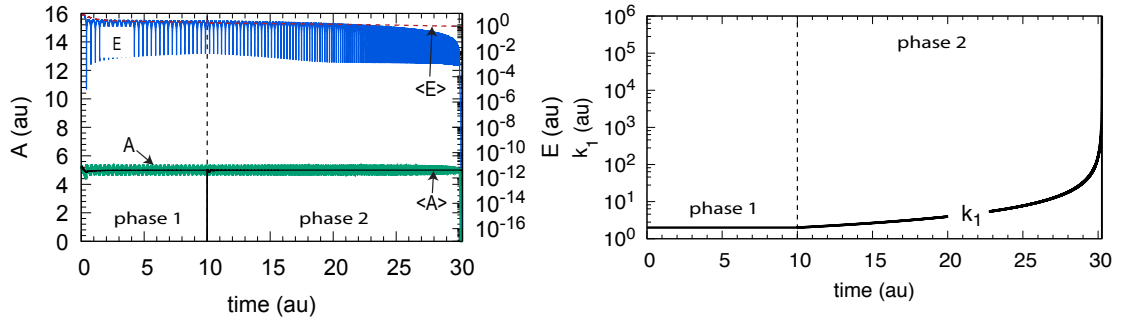


FIGURE 4.18: Controller motif 2 with hyperbolic increase in k_1 by Equation 4.10 and multisite inhibition $n=4$. Left panel: Concentrations of A and E as a function of time while perturbation increases linear and average concentrations of $\langle A \rangle$ and $\langle E \rangle$. In the first phase which is 10 time units long the $k_1=5$ and after that is increases hyperbolic until the infinity limit is reached in phase 2 at total time : 18.01. Other concentrations are $K_I=1$, $k_2=1 \times 10^5$, $k_3=5 \times 10^1$, $k_4=1 \times 10^1$, $K_M=1 \times 10^{-6}$, $n = 4$. Initial concentrations are: $A_0 = 1.5, E_0 = 2.1$. The right panel shows the concentration of k_1 as function of time.

4.5.2 Time dependent perturbation of controller motif 2 with C

We wanted to see how the increase in compensatory flux k_2 is affecting the behaviour of the controller. As we have seen in the Figure 4.14 (panel b) when we have the controller motif 2 (Figure 1.4) we can avoid the breakdown by increasing the compensatory flux. So the same effect is to be expected when adding the variable C which activates the synthesis of A by positively affecting the compensatory flux k_2 . The controller motif 2 with variable C is shown on the Figure 4.4. The Equations for oscillatory behaviour are Equation 1.1 for calculating the concentration of A and Equation 1.7 for calculating the concentration of E . As for C it is calculated using the Equation 4.4.

Now we have tested this controller in cases when perturbation (value of k_1) is increasing linearly, stepwise, exponentially and hyperbolic. We as well assume that E can bind to 4 binding sites on transporter or enzyme.

When we test the controller against the linear increase in the k_1 the controller is able to keep the average value of A at the A_{set} . The controller is oscillating around the average value. The frequency of oscillations are increasing with linear increase. This is shown on the Figure 4.19. In comparison to the controller motif without C with linear increase (Figure 4.16) we observe that both controllers are able to keep the $\langle A \rangle$ at the A_{set} . We also observe that in the case of controller with C the $\langle E \rangle$ is also kept at the steady state and has a higher concentration while it is decreasing in concentration for the controller without C (Figure 4.16).

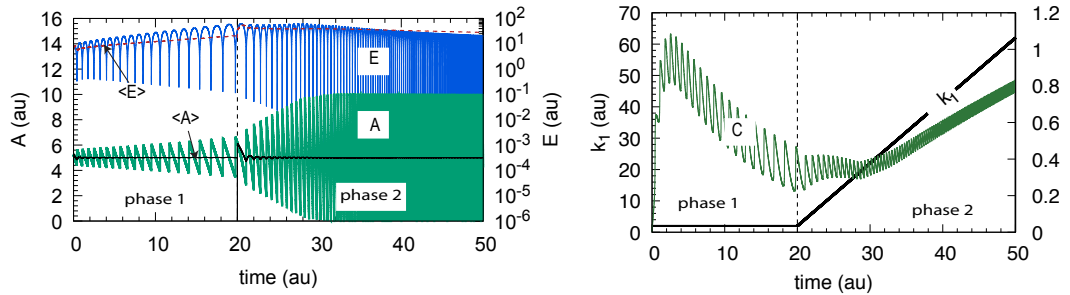


FIGURE 4.19: Controller motif 2 with C , linear increase in k_1 by Equation 4.8 and multisite inhibition $n=4$. Left panel: Concentrations of A and E as a function of time while perturbation increases linearly and average concentrations of $\langle A \rangle$ and $\langle E \rangle$. In the first phase which is 20 time units long the k_1 is constant $k_1=2$ and then it starts to increase linearly by Equation 4.8 in the phase 2 which is 30 time units long. Other concentrations are $K_I=0.1$, $k_2=1 \times 10^5$, $k_3=5 \times 10^2$, $k_4=1 \times 10^2$, $K_M=1 \times 10^{-6}$, $n = 4$. Initial concentrations are: $A_0 = 5.2, E_0 = 6.9, C_0 = 1.8 \times 10^{-3}$. The right panel shows the concentration of k_1 and C as function of time.

For the stepwise increase in k_1 we observe that the frequency in oscillations in all phases is smaller when we are having the C in the system. It is as well observed that the concentration of the E is higher than in the controller without C . When we look at the right panel of the Figure 4.20 we observe that C is decreasing with the increase in perturbation. The frequency of oscillations is increasing and the amplitude is decreasing. So in the phase 3, when the k_1 increases mostly the C reached steady state and oscillates.

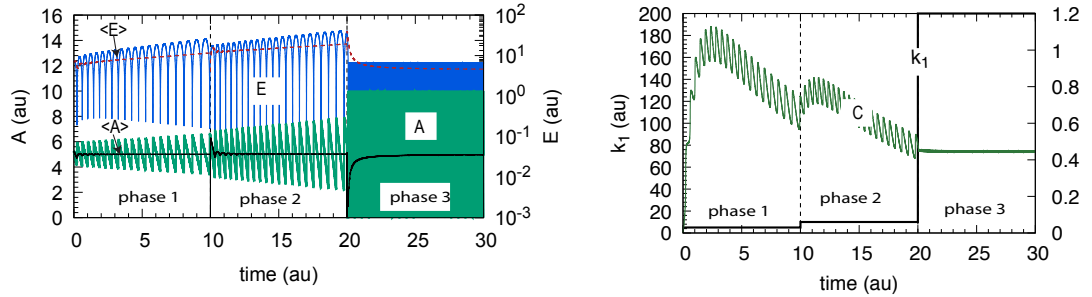


FIGURE 4.20: Controller motif 2 with C , stepwise increase in k_1 and multisite inhibition $n=4$. All phases are 10 time units long and the k_1 in three phases are: In phase 1: $k_1 = 5$; In phase 2: $k_1 = 10$; In phase 3: $k_1 = 200$. Left panel: Concentrations of A and E as a function of time while perturbation increases stepwise and average concentrations of $\langle A \rangle$ and $\langle E \rangle$. Other concentrations are $K_I=0.1$, $k_2=1 \times 10^5$, $k_3=5 \times 10^2$, $k_4=1 \times 10^2$, $K_M=1 \times 10^{-6}$, $n = 4$. Initial concentrations are: $A_0 = 5.2, E_0 = 6.9, C_0 = 1.8 \times 10^{-3}$.

The right panel shows the concentration of k_1 and C as function of time.

For the exponential increase the controller with exponential increase the controller is as well able to keep the $\langle A \rangle$ at A_{set} point. When comparing to the controller motif without C (Figure 4.17) we observe that the $\langle E \rangle$ is higher in both phases when we have the C and is not decreasing as much as in the first situation (without C). When looking at the right panel of the Figure 4.21 we see that the C oscillates and is decreasing in the first phase while it starts to exponentially increasing when k_1 start to increase. This result was compared using MATLAB and can be seen on the Figure B.6 in B.6.

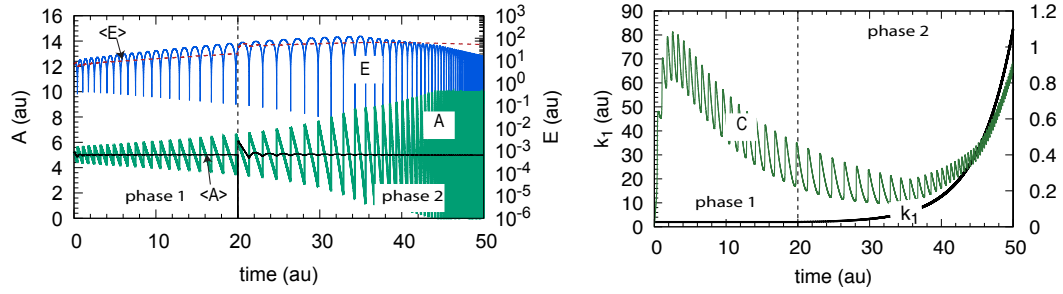


FIGURE 4.21: Controller motif 2 with C , exponential increase in k_1 by Equation 4.9 and multisite inhibition $n=4$. Left panel: Concentrations of A and E as a function of time while perturbation increases linear and average concentrations of $\langle A \rangle$ and $\langle E \rangle$. In the first phase which is 20 time units long the $k_1 = 2$ and after that is increases exponentially in the phase 2 which is 30 time units long. Other concentrations are $K_I=0.1$, $k_2=1 \times 10^5$, $k_3=5 \times 10^2$, $k_4=1 \times 10^2$, $K_M=1 \times 10^{-6}$, $n = 4$. Initial concentrations are: $A_0 = 5.2, E_0 = 6.9$ and $C_0 = 1.8 \times 10^{-3}$. The right panel shows the concentrations of k_1 and C as function of time.

Further we have tested the controller with C against the hyperbolic increase in k_1 . We observe that the controller is as expected able to keep the $\langle A \rangle$ at A_{set} until the infinity limit is reached. When compared to the controller without C with the hyperbolic increase (Figure 4.18 we observe the same trend only that concentration of $\langle E \rangle$ is much higher then without C .

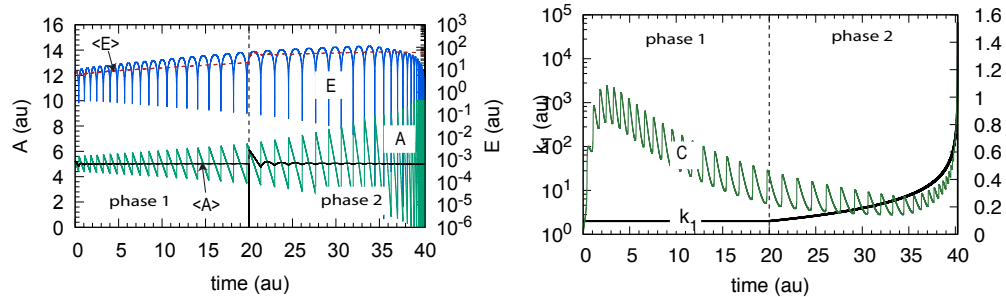


FIGURE 4.22: Controller motif 2 with C , hyperbolic increase in k_1 by Equation 4.10 and multisite inhibition $n=4$. Left panel: Concentrations of A and E as a function of time while perturbation increases hyperbolic and average concentrations of $\langle A \rangle$ and $\langle E \rangle$. In the first phase which is 20 time units long the $k_1 = 2$ and after that is increases hyperbolic in the phase 2 until the infinity limit is reached at time=40.24939. Other concentrations are $K_I=0.1$, $k_2=1 \times 10^5$, $k_3=5 \times 10^2$, $k_4=1 \times 10^2$, $K_M=1 \times 10^{-6}$, $n = 4$. Initial concentrations are: $A_0 = 5.2, E_0 = 6.9$ and $C_0 = 1.8 \times 10^{-3}$. The right panel shows the concentrations of k_1 and C as function of time.

Chapter 5

Conclusion and Outlook

Controller motifs like the one presented here can be used in order to remodel some existing biological systems as well as it can be used to explain and shed a light to the newly discovered ones. Beside this application in direct biology, this research can help in future work on the controller motifs by for example directing the researcher while they investigate new controller motifs.

The aim of this thesis was to stop the breakdown of the m2-controller while still keeping the same properties of controller, and this was achieved by incorporating the variable C with second order autocatalysis as illustrated on the Figure 4.5. This controller is able to withstand all types of time dependent perturbations (linear, stepwise, exponential and even hyperbolic). E itself gets homeostatic regulated as well and reaches steady state which corresponds to the calculated E_{set} values. We have as well followed the effect the increase in k_1 has on the concentration of C and we observe that when we have the second order autocatalysis in C , concentration of C follows the increase in k_1 closely.

We have taken the research one step further and looked into the oscillatory behavior of the m2-controller 1.4. By modifying controller as explained in the section 1.5 the controller oscillated around the setpoint. Implementing the C in the system lead to the decrease in frequency of oscillations and the controller was less stressed.

Computational biology, is underestimated. Most of the research around biological systems is focused on the question: What is it, and what is it made of? But, I think that it is likewise important to look into how the different species behave and interact.

Although the m2-feedback loop including C has so far not been found as an biological example, it appears interesting to search for it. One may wonder whether nature as found this solution during the course of evolution.

Bibliography

- [1] N. Wiener. *Cybernetics: or Control and Communication in the Animal and the Machine. Second Edition.* The MIT Press, Cambridge, Massachusetts, 1961.
- [2] C Bernard. *Leçons sur les phénomènes de la vie communs aux animaux et aux végétaux* (Paris: Jb bailliere et fils). 1878.
- [3] Claude Bernard. *An introduction to the study of experimental medicine.* Dover Publications, 1957.
- [4] WB Cannon. Organization for Physiological Homeostasis. *Physiol. Rev.*, 9:399–431, 1929.
- [5] Langley, LL, editor. *Homeostasis. Origins of the Concept.* Dowden, Hutchinson & Ross, Inc., Stroudsboung, Pennsylvania, 1973.
- [6] L. Sherwood. *Human Physiology: From Cells to Systems.* Cengage Learning, 2015. ISBN 9781305445512. URL https://books.google.no/books?id=_i5BBAAAQBAJ.
- [7] Valerie Anne Galton, Emily T. Wood, Emily A. St. Germain, Cheryl-Ann Withrow, George Aldrich, Genevieve M. St. Germain, Ann S. Clark, and Donald L. St. Germain. Thyroid Hormone Homeostasis and Action in the Type 2 Deiodinase-Deficient Rodent Brain during Development. *Endocrinology*, 148(7):3080–3088, 07 2007. ISSN 0013-7227. doi: 10.1210/en.2006-1727. URL <https://doi.org/10.1210/en.2006-1727>.
- [8] Ellen L O’Dea, Derren Barken, Raechel Q Peralta, Kim T Tran, Shannon L Werner, Jeffrey D Kearns, Andre Levchenko, and Alexander Hoffmann. A homeostatic model of κb metabolism to control constitutive $\text{nf-}\kappa\text{b}$ activity. *Molecular systems biology*, 3(1), 2007.
- [9] T Drengstig, IW Jolma, XY Ni, K Thorsen, XM Xu, and P Ruoff. A basic set of homeostatic controller motifs. *Biophys J*, 103(9):2000–2010, 2012.
- [10] T. M. Yi, Y. Huang, M. I. Simon, and J. Doyle. Robust perfect adaptation in bacterial chemotaxis through integral feedback control. *PNAS*, 97(9):4649–53, 2000.

-
- [11] X.Y. Ni, T. Drengstig, and P. Ruoff. The control of the controller: Molecular mechanisms for robust perfect adaptation and temperature compensation. *Biophys J*, 97():1244–53, 2009.
- [12] I. W. Jolma, X. Y. Ni, L. Rensing, and P. Ruoff. Harmonic oscillations in homeostatic controllers: Dynamics of the p53 regulatory system. *Biophys J*, 98(5):743–52, 2010.
- [13] Oren Shoval, Lea Goentoro, Yuval Hart, Avi Mayo, Eduardo Sontag, and Uri Alon. Fold-change detection and scalar symmetry of sensory input fields. *Proceedings of the National Academy of Sciences*, 107(36):15995–16000, 2010.
- [14] T. Drengstig, X.Y. Ni, K. Thorsen, I.W. Jolma, and P. Ruoff. Robust adaptation and homeostasis by autocatalysis. *J Phys Chem B*, 116:5355–5363, 2012.
- [15] Corentin Briat, Christoph Zechner, and Mustafa Khammash. Design of a synthetic integral feedback circuit: dynamic analysis and dna implementation. *ACS Synthetic Biology*, 5(10):1108–1116, 2016.
- [16] Corentin Briat, Ankit Gupta, and Mustafa Khammash. Antithetic integral feedback ensures robust perfect adaptation in noisy biomolecular networks. *Cell Systems*, 2(1):15–26, 2016.
- [17] Stephanie K Aoki, Gabriele Lillacci, Ankit Gupta, Armin Baumschlager, David Schweingruber, and Mustafa Khammash. A universal biomolecular integral feedback controller for robust perfect adaptation. *Nature*, 570(7762):533–537, 2019.
- [18] Gunhild Fjeld, Kristian Thorsen, Tormod Drengstig, and Peter Ruoff. The performance of homeostatic controller motifs dealing with perturbations of rapid growth and depletion. *The Journal of Physical Chemistry B*, 121:6097–6107, 2017.
- [19] D Lloyd, MA Aon, and S Cortassa. Why Homeodynamics, Not Homeostasis? *The Scientific World*, 1:133–145, 2001.
- [20] M. C. Moore-Ede. Physiology of the circadian timing system: Predictive versus reactive homeostasis. *Am. J. Physiol.*, 250:R737–52, 1986.
- [21] JC Dunlap, JJ Loros, and PJ DeCoursey. *Chronobiology. Biological Timekeeping*. Sinauer, Sunderland, MA, 2004.
- [22] A. Goldbeter. *Biochemical Oscillations and Cellular Rhythms*. Cambridge University Press, Cambridge, 1996.
- [23] M. Maroto and N.A.M. Monk. *Cellular oscillatory mechanisms*. Springer, New York, 2008.

- [24] T.Y.C. Tsai, Y.S. Choi, W. Ma, J.R. Pomeroy, C. Tang, and J.E. Ferrell. Robust, Tunable Biological Oscillations from Interlinked Positive and Negative Feedback Loops. *Science*, 321(5885):126–129, July 2008.
- [25] Kristian Thorsen, Oleg Agafonov, Christina H Selstø, Ingunn W Jolma, Xiao Y Ni, Tormod Drengstig, and Peter Ruoff. Robust concentration and frequency control in oscillatory homeostats. *PloS one*, 9(9):e107766, 2014.

Appendix A

Multisite inhibition with different K_I values

In the first part of the Results sections we have tested effect of different values of K_I on the controller motif 2. We observed that the $K_I=1x10^{-3}$ lead to the best results, the controller lifetime was not affected but the aggressiveness of controller was increased as well as its ability to hold A at A_{set} . This can be seen on the Figure 4.1. We have further tested the controller for the multisite inhibition but we choose to use $K_I=0.1$. We have tested the controller with the $K_I=1x10^{-3}$ and the result is presented on the Figure A.1. Here we tested the multisite inhibition effect on the controller and compared it to the result for the controller for $n=4$ binding sites and when $K_i=0.1$ (Blue dashed line presents the E and blue line presents the A .) We see that the controller with $K_I=0.1$ (blue) holds the A at the A_{set} longest. Controller is maybe less aggressive than the E_4 but the difference is not to big for us to change to lower K_I value which is why we are continuing with $K_I=0.1$.

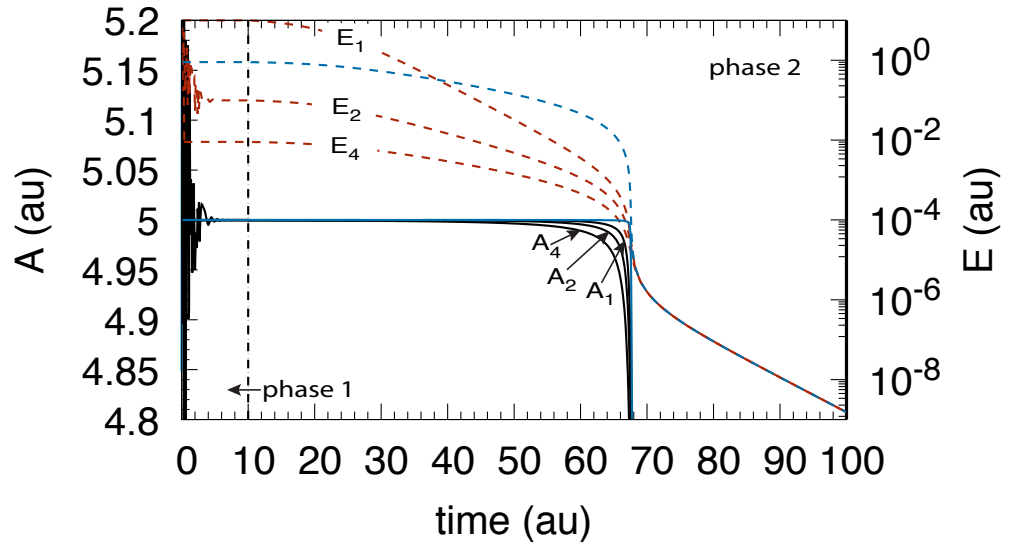


FIGURE A.1: Testing the multisite inhibition with $K_I=1x10^{-3}$, n is the number of inhibition sites tested. E_1 and A_1 are for $n=1$, E_2 and A_2 are for $n=2$, E_4 and A_4 are for $n=4$. k_1 increases exponentially in the phase 2, $k_2=1x10^5$, $k_3=5x10^3$, $k_4=1x10^3$, $K_I=1x10^{-3}$ and $K_M=5x10^3$. Initial concentrations are: $A_0=5.0$, $E_0=9.9$ and $C_0=1.0$. The blue lines are the result for $n=4$ from the Figure 4.1.

Appendix B

Checking the results using MATLAB

In this section we have compared some of the results run in Fortran, in the MATLAB. These files will be available as the Supplementary files as well.

B.1 Controller motif 2 without C and with exponential increase

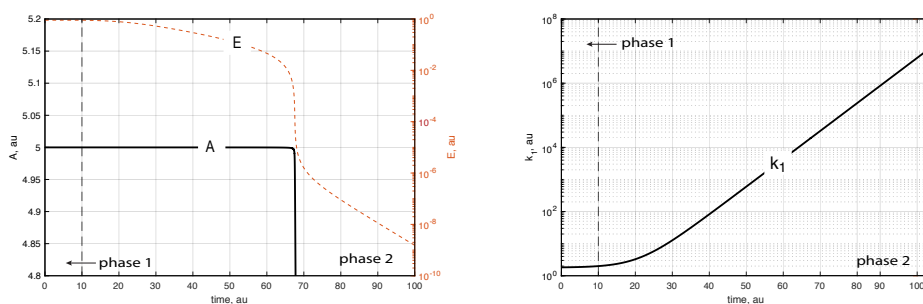


FIGURE B.1: Comparing the results presented on the Figure 4.2 using MATLAB. The $n=4$ and all concentrations are as described under the Figure.

B.2 Controller motif 2 with C and exponential increase

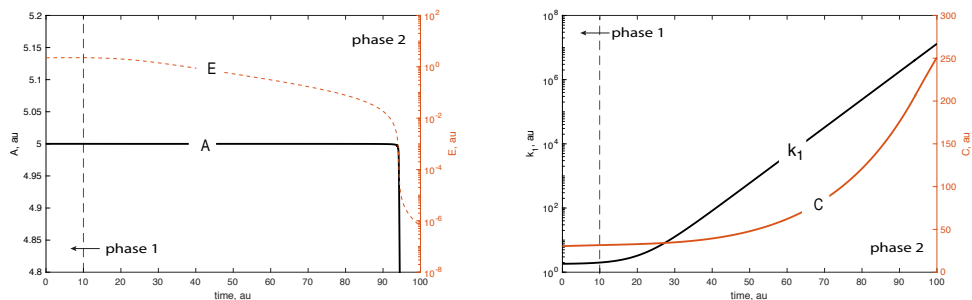


FIGURE B.2: Comparing the results presented on the Figure 4.4 using MATLAB. Given result is comparing the result when $k_5=1.0$ and $k_5=0.1$. Other rate constants are the same as on the Figure we are comparing it to. Here on the right panel we have the C value for the controller as well as we show that the k_1 is increasing exponentially.

B.3 Controller motif 2 with C and first order autocatalysis and exponential increase

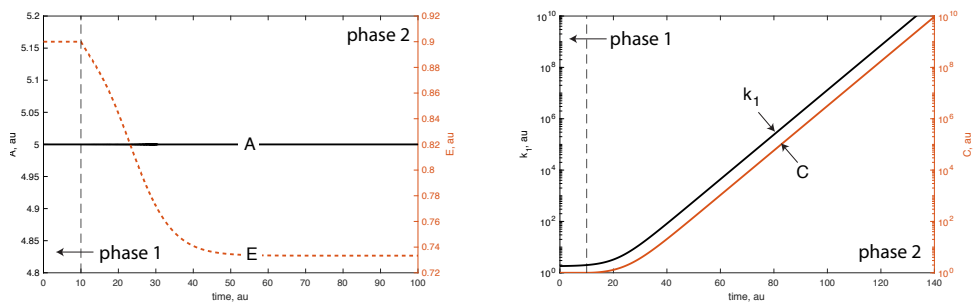


FIGURE B.3: Comparing the results presented on the Figure 4.8 using MATLAB. All initial values and the rate constants are the same as in the Figure 4.8 .

B.4 Controller motif 2 with C and second order autocatalysis

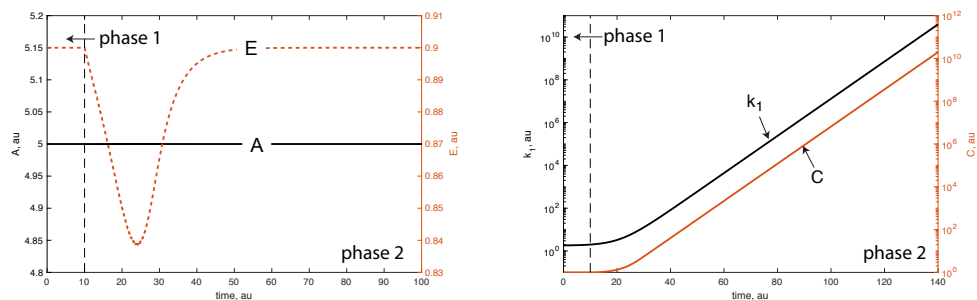


FIGURE B.4: Comparing the results presented on the Figure 4.12 using MATLAB. All initial values and the rate constants are the same as in the Figure 4.12 .

B.5 Oscillatory Controller motif 2 with exponential increase

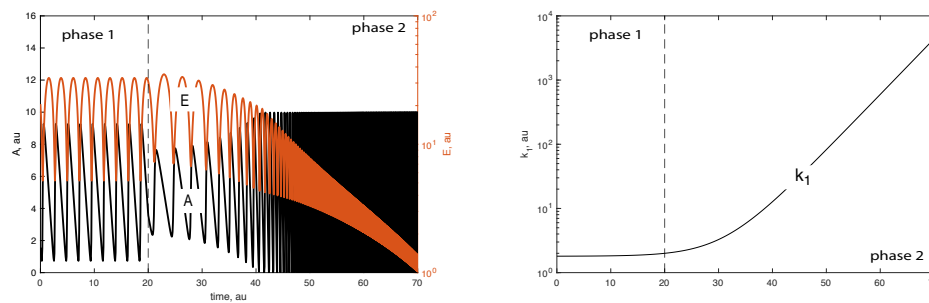


FIGURE B.5: Comparing the results presented on the Figure 4.17 using MATLAB. All initial values and the rate constants are the same as in the Figure 4.17.

B.6 Oscillatory Controller motif 2 with C and exponential increase

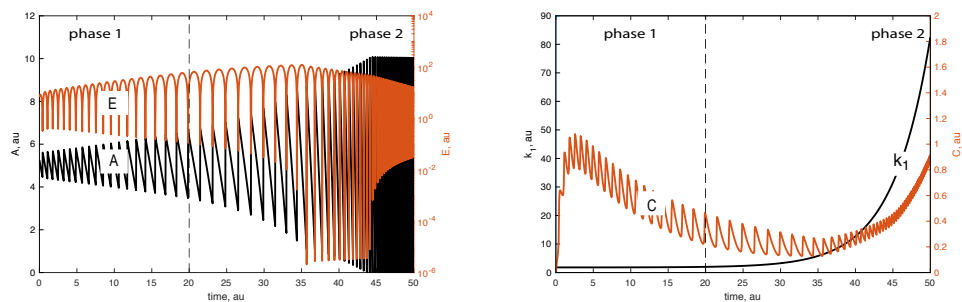


FIGURE B.6: Comparing the results presented on the Figure 4.21 using MATLAB. All initial values and the rate constants are the same as in the Figure 4.21.

Appendix C

Fortran and MATLAB program parts

In this section I present important parts of the Fortran and MATLAB program that are varied in order to get the results. For illustration I am using the part of the Fortran program used to obtain the results presented on the Figure 4.12 and part of the MATLAB program used to get the result presented on the Figure B.4.

The Fortran file is presented on the Figure C.1. This files are available as supplementary files as well.

a

```

C Enter loop calling LSODE
200      CONTINUE

      IF (NTIMES.EQ.2) THEN
!      K1=K1_1+1000.0*(TIMSEQ-TOUTF1)!linear increase;
!      IF (K1.GE.NEWK1) K1=NEWK1
      K1=K1_1+0.2*(DEXP(0.2*(TIMSEQ-TOUTF1))-1.0D+00 ) !exponential increase
!      K1=40.5/((40.5/K1_1) -(TIMSEQ-TOUTF1)) !hyperbolic increase
!      K1DOT=40.5/((TIMSEQ-21.25)**2)
!      GAMMA=(K1DOT*((KI+Y(2))**2))/(K2*KI*K4)
!      K1_2=K1
!      ASET=K3/K4
!      ASS=(ASET)/(1+GAMMA)
      ENDIF

```

b

```

SUBROUTINE FEX (NEQ, T, Y, YDOT)
DOUBLE PRECISION T, Y, YDOT
DOUBLE PRECISION K1,K2,K3,K4
DOUBLE PRECISION K5,K6,K7,K8,K11,KI,KM

DIMENSION Y(7),YDOT(7)
COMMON /RATCON/K1,K2,K3,K4,K5,K6,K7,K8,K11,KI,KM

YDOT(1)=-K1*Y(1)+K2*KI/((KI+Y(2))*Y(2))
YDOT(1)=-K1*Y(1)+K2/((1.0+(Y(2)/KI))*1.0)
YDOT(1)=-K1*Y(1)+K2*Y(5)/((1.0+(Y(2)/KI))*2.0) !allosteric inhibition n=2 m2ac-59
YDOT(1)=-K1*Y(1)+K2*Y(5)/((1.0+(Y(2)/KI))*4.0) !allosteric inhibition n=4 m2ac-60-71,
YDOT(1)=-K1*Y(1)/(KM+Y(1))+K2*Y(5)/((1.0+(Y(2)/KI))*4.0) !oscillatory homeostasis med n=4
allosteric inhibition n=4

YDOT(1)=-K1*Y(1)+K2*Y(5)/((1.0+(Y(2)/KI))*1.0) !normal inhibition n=1 m2ac-58; -72
YDOT(2)=K4*Y(1)-K3*Y(2)/(KM+Y(2))
YDOT(3)=0.0D+0
YDOT(4)=0.0D+0
YDOT(5)=K5*KI/(KI+Y(2))-K6*Y(5) !species C without autocatalytic generation, m2ac-61,..-71
YDOT(5)=K5*KI*Y(5)/(KI+Y(2))-K6*Y(5) !autocatalytic generation of C
YDOT(5)=(K5*KI*(Y(5)**2.0))/(KI+Y(2))-K6*Y(5)*Y(5) !second-order autocatalytic generation of C
|DOT(5)=0.0D+0 !no generation of C

RETURN
END

```

FIGURE C.1: The selected part of the Fortran program used to obtain the result presented on the Figure 4.12. In the panel a of the Figure we can see the LSODE loop of the program which here defines the perturbation. The highlighted is the Equation 4.9 used to calculate k_1 in the case of exponential increase. In the panel b of the Figure we can see all the rate equations used in this case.

a

```

1 function dy=m2zo_C2ndaut(T,y,k);
2
3 dy=zeros(3,1);
4
5 % assignments motif 2 controller (Fig. 12):
6 % y(1) <-> A
7 % y(2) <-> E
8 % y(3) <-> C
9
10
11 %exponential increase of k1 from t>= 10.0:
12 if T >= 10.00
13     k(1)=2.0 + 0.2*(exp(0.2*(T-10.0))-1);
14 end
15
16
17
18 dy(1)=-k(1)*y(1)+k(2)*y(3)/((1.0+(y(2)/k(7)))^4.0);
19 dy(2)=k(4)*y(1)-k(3)*y(2)/(k(8)+y(2));
20 dy(3)=k(5)*k(7)*y(3)*y(3)/(k(7)+y(2))-k(6)*y(3)*y(3);
21

```

b

```

9 % fortran <=> matlab
10 %-----
11 % K1=2.0    <=> k(1) perturbation
12 % K2=1.e+5 <=> k(2) compensatory flux
13 % K3=5.e2  <=> k(3) degradation constant (Vmax) of E
14 % K4=1.e2  <=> k(4) synthesis of E induced by A
15 % K5=10.0  <=> k(5) rate constant for generating C by 2nd-order process)
16 % K6=1.0   <=> k(6) rate constant for removing C by 2nd-order process
17 % KI=0.1   <=> k(7) inhibition constant
18 % KM=1.e-6 <=> k(8) KM, MM-degradation of E
19
20 %vector of rate constant values
21 k =[2 1.e5 5.e2 1.e2 10.0 1.0 0.1 1.e-6];
22
23 % total simulation time
24 T=[0 140.00];
25
26
27 % assignments motif 2 zero-order controller
28 % y(1) <-> A
29 % y(2) <-> E
30 % y(3) <-> C
31
32
33
34
35 % initial concentrations:
36 y0=[5.0 0.9 1.0];
37
38
39 % options for numerical integration
40 options = odeset('RelTol',1.0e-6,'absTol',1e-9,'MaxStep',0.01);
41 % Solve model
42
43 [T, Y]=ode15s(@m2zo_C2ndaut,T,y0,options,k);
44
45 %the variation of k1 in the second phase is recalculated for plotting
46 k1=2.0 + 0.2*(exp(0.2*(T-10.0))-1); % t > 10

```

FIGURE C.2: The selected part of the MATLAB program used to obtain the result presented on the Figure B.4. In the panel a of the Figure we can see the assignments given for the program together with the Equations for calculations of concentrations of A , E and C . In the panel b of the Figure we can see all the rate constants, and numerical integration's used in this case.